REVIEW ARTICLE | FEBRUARY 05 2026

Recent developments and perspectives on laser-driven neutron sources (LDNSs) FREE

T. Gutberlet ; M. Bleuel ; T. Brückel ; L. G. Butler ; C. Guerrero ; T. T. Jäger ; G. Muhrer ; S. Scheuren ; A. Schreyer ; S. C. Vogel ; K. Zeil

Rev. Sci. Instrum. 97, 021501 (2026)
https://doi.org/10.1063/5.0289016

Review of Scientific Instruments REVIEW pubs.aip.org/aip/rsi

Recent developments and perspectives on laser-driven neutron sources (LDNSs)

Cite as: Rev. Sci. Instrum. 97, 021501 (2026); doi: 10.1063/5.0289016
Submitted: 24 July 2025 • Accepted: 24 December 2025 •
Published Online: 5 February 2026

T. Gutberlet,[1,a] M. Bleuel,[2] T. Brückel,[1] L. G. Butler,[2] C. Guerrero,[3] T. T. Jäger,[4] G. Muhrer,[5] S. Scheuren,[4] A. Schreyer,[6] S. C. Vogel,[7] and K. Zeil[8]

AFFILIATIONS

[1] Forschungszentrum Jülich GmbH, 52425 Jülich, Germany
[2] Louisiana State University, Baton Rouge, Louisiana 70803, USA
[3] Universidad de Sevilla, 41012 Sevilla, Spain
[4] TU Darmstadt, 64289 Darmstadt, Germany
[5] ESS AB, 224 84 Lund, Sweden
[6] Helmholtz Zentrum Hereon, 21502 Geesthacht, Germany
[7] Los Alamos National Laboratory, Los Alamos, New Mexico 87545, USA
[8] Helmholtz Zentrum Dresden-Rossendorf, 01328 Dresden, Germany

[a] **Author to whom correspondence should be addressed:** t.gutberlet@fz-juelich.de

ABSTRACT

Since their discovery over 90 years ago, neutrons have become one of the premier tools in the study of the structure and dynamics of matter and materials. The main nuclear processes to generate a large number of free neutrons are fusion, fission, and spallation, which have been well established for using neutrons in broad areas of physics, material science, engineering, life sciences, and elsewhere. The vast majority of experiments that use neutrons as a probe require a directional, well-collimated beam of neutrons. Over the years, methods have been developed to deliver such neutron beams sufficiently, but it is still much desired to improve the efficiency of neutron sources. With the advent of high-powered lasers, laser-driven neutron sources suggest an attractive possibility. Laser photons can be converted to neutrons by accelerating particles (electrons, protons, and deuterons) and then either utilize hard x rays from, for example, electron acceleration to create photoneutrons or nuclear reactions, such as deuteron break-up. The maturity of such processes in recent years might have reached a state where such neutron sources are becoming useful and beneficial to the neutron community. In the present report, the current state-of-the-art of a laser-driven neutron source and its future development for neutron applications are presented, and existing sources are described. The basic physical principles of laser-driven neutron production and the current state-of-the-art of production techniques are outlined. The potential developments and the role of such sources in the landscape of neutron sources in the future are critically commented on.

I. INTRODUCTION

Since their discovery over 90 years ago, neutrons have become one of the premier tools in the study of the structure and dynamics of matter and materials, with unique abilities to probe bulk material properties, magnetism, and their exceptional sensitivity to light elements, in particular, hydrogen. The main nuclear processes to generate a large number of free neutrons are fusion,[1] fission,[2] and spallation,[3] which are commonly applied in neutron generators, research reactors, and spallation neutron sources. Nuclear reactors and accelerator-based spallation neutron sources are exploited heavily worldwide at large neutron user facilities offering broad access for science and industry. A recent review article[4] provides an up-to-date overview of those neutron sources and their application in research with neutrons.

The vast majority of experiments that use neutrons as a probe require a directional, well collimated beam of neutrons. In order to generate these collimated beams, in both cases, fission and

spallation, one has to deal with inherent 4 π processes, wasting most of the produced neutrons. Currently, accelerator-driven neutron sources are being designed as an advancement of Compact Accelerator-driven Neutron Sources (CANSs). These High Current Accelerator-driven Neutron Sources (HiCANSs) do not aim at the highest source strength but instead at a more efficient neutron provision for beam line instruments to minimize neutron waste.[4]

Over the years, methods have been developed to reduce this inefficiency via neutron guide systems or complex moderator reflector assemblies. However, these techniques come with not insignificant costs. In addition, the ability of neutrons to penetrate materials deeply, which allows one to study bulk properties, is not only an advantage, but, on the downside, causes a much more challenging radiation safety environment than, for example, photons. Because of this, neutron sources come with a substantial infrastructure and operational cost. A proton accelerator of a spallation source or a nuclear reactor is a giant investment, a cost that is much higher than the investment for an off the shelf lab-based x-ray source or a neutron generator, and therefore not easily affordable for most universities and research labs.

Laser-driven neutron sources (LDNSs) could present an option for future affordable neutron sources for certain applications. LDNSs have exceptionally short pulse duration and highly directional pulse characteristics that are very hard to achieve with conventional particle accelerators or fission reactors. This makes LDNSs, in particular, for time-of-flight methods interesting, where ~1 ns pulses are needed using neutron energies where the moderation does not dominate directional characteristics, nor the time resolution. The technological maturity seems to have reached a state where such neutron sources could become useful and have been referred to in recent reviews.[5,6]

In this report, the current state-of-the-art of laser-driven neutron sources and their potential in future development for neutron applications will be discussed. The basic physical principles of laser-driven neutron production and the state-of-the-art of production techniques are outlined. The applications of laser-driven neutron sources will be presented, and existing sources described and the potential developments and the role of such sources in the landscape of neutron sources in the future are critically commented on. The report is based on discussions during a workshop by the League of advanced European Neutron Sources (LENS) held in 2023 at the European Spallation Source (ESS) in Lund, Sweden.

II. LASER-DRIVEN NEUTRON PRODUCTION

A. Neutron generating reactions

Only a few basic nuclear reaction mechanisms produce neutrons when accelerated particles are applied: elastic break-up, complete fusion (compound formation followed by neutron emission), incomplete fusion (inelastic break-up or deuteron stripping), and photoneutron generation.

1. Elastic break-up

Elastic break-up of an atomic nucleus occurs in the vicinity of a converter atom, which does not partake in the reaction. Deuteron break-up is one of the most commonly referred reactions in the realm of neutron generation below 100 MeV. Deuterons dissociate in the Coulomb potential of converter atoms, thus producing a proton and a neutron. The generated neutron beam has a continuous energy spectrum similar to that of the incoming ion beam and is forward-directed due to conservation of momentum. For materials with low Z, such as beryllium and lithium, the Coulomb potential is rather weak in comparison to the ion energies. This, on the one hand, explains the low break-up cross section and, on the other hand, enables interactions via the strong nuclear force as the deuteron can approach closer to the nucleus. This increases the likelihood of the deuteron stripping processes.

2. Complete and incomplete fusion

When a deuteron and a target atom form a short-lived compound state, complete fusion occurs that then decays to a more stable atom through emission of a neutron either before or after equilibration.

A hybrid of elastic break-up and complete fusion is termed incomplete fusion, whereby inelastic scattering of the incoming particles allows the projectile to knock out nucleons or break up the target nucleus into fragments.

The generation of dense hot deuteron (D^+) ion beams and realization of compact neutron sources through interaction of several ultra-intense femtosecond lasers with a deuterated pitcher–catcher target have been demonstrated. Here, the laser fields are enhanced in the target surface layer when the laser pulses impinge on the front surface of the pitcher layer. As a result, the temperature of the laser-driven hot electrons is significantly increased, and a strong target-normal sheath acceleration (TNSA) field is induced for driving the D^+ ions to higher temperatures and densities. It is found that the maximum neutron production rate per unit volume is considerably higher than that from a single pulse of the same total energy.[7]

Fusion neutrons are generated in laser produced plasmas by large-scale laser facilities, usually in the context of inertial confinement fusion (ICF) research. The fusion yield in such experiments can be substantial; for example, nearly 5×10^9 DD fusion neutrons were produced in an ICF implosion by the Nova laser at the Lawrence Livermore National Laboratory (LLNL) using about 30 kJ of laser energy.[8] Up to 6×10^4 thermonuclear DD fusion neutrons have been observed from the irradiation of solid, deuterated plastic targets by a 500 J, 5 ps laser.

When large clusters (>1000 atoms per cluster) are ionized, electrons undergo rapid collisional heating for a short time (<1 ps) before the cluster disassembles in the laser field. The laser rapidly heats the electrons to a non-equilibrium state (with mean energies of many keV). The escape of these hot electrons from the cluster produces a strong radial electric field, which accelerates the cluster ions. The deposited energy is therefore transferred from the light electrons to the more massive ions. The consequence is that the cluster can very efficiently absorb laser energy (often many tens of keV per atom in the cluster), and this energy is ultimately released in ion kinetic energy when the heated cluster explodes isotropically. If the ion energy is high enough (greater than a few MeV), D^+D nuclear-fusion events occur with high probability.[8]

In early experiments in 1999, about 10^5 n/pulse were produced. This method has been improved, resulting in a yield of 10^7 n/pulse at the Texas Petawatt Laser that can deliver 120 J in a fs pulse duration. The source size in these experiments is of the order of only a few tens of micrometers (which is the focal region in the cluster volume).

3. Photoneutron generation

Photoneutron generation occurs when the photon energy exceeds the nuclear binding energy of a loosely bound neutron.[9] Neutron generation via high-energy electrons involves directing electrons into high-Z targets, such as uranium, lead, or tungsten, inducing the emission of bremsstrahlung gammas. These gammas interact with target nuclei, leading to photo-nuclear reactions or photo-fission events.[10] When photon energies surpass the neutron binding energy, processes such as the giant dipole resonance or the quasi-deuteron effect[11] with subsequent neutron emission are initiated. In the giant dipole resonance regime (up to 20–30 MeV), neutron production occurs through photon induced oscillations of nuclei, with isotropic neutron emission and neutron energy peaking around 1 MeV. Beyond the giant dipole resonance, at photon energies exceeding 20–30 MeV, neutron generation occurs via direct reactions such as the quasi-deuteron effect. The quasi-deuteron effect describes the interaction of photons with a neutron–proton pair inside the nucleus, rather than the nucleus as a whole.[12] Neutrons generated from this reaction commonly have energies between the binding energy and half the energy of the incoming photon. Thus, for high-energy electrons, a tail component with high energies can be observed in the neutron spectrum. Another neutron generating reaction process is photo-fission, where the photon induces the fission of the target nucleus.[10,13] Materials with high photo-fission cross sections include thorium, uranium, and other transuranium elements.[13,14]

B. Physical processes

1. Target-normal sheath acceleration (TNSA)

Laser photons can release neutrons by accelerating particles (electrons, protons, and deuterons) and then either using hard x rays from, for example, electron acceleration to create photoneutrons or inducing nuclear reactions, such as deuteron break-up in so-called pitcher–catcher methods. In the latter, a thin (100 nm–1 μm) target is hit by a laser beam, heating the target electrons to MeV temperatures and accelerating them via the pondermotive force and other mechanisms toward the rear side of the target. There, they build an electron-sheath behind the target, which generates an electric field through the charge separation. This electric field is in the range of TeV/m, and the field ionizes the ions at the rear surface, which are subsequently accelerated to tens of MeV in the direction normal to the target surface. The process is illustrated in Fig. 1 and is called target-normal sheath acceleration (TNSA), which was first demonstrated by Hatchett *et al.* [15,16]

In solid TNSA targets, the rear surface of the target is coated with a contamination layer comprised of water and hydrocarbons, which accumulate due to exposure to air. This layer contains a high concentration of hydrogen atoms. Considering that protons have the highest charge-to-mass ratio, they become the most efficiently accelerated particles in this configuration. Within this mechanism, the achievable maximum proton energy can mainly be boosted by progressively increasing the laser energy coupled into the plasma. Alternative acceleration mechanisms utilize field structures that drive protons in a more coherent manner to further increase achievable maximum energies. Recent experiments demonstrated that the superposition or cascade of multiple acceleration mechanisms at target densities close to the relativistic transparency regime can result in energies around or even well beyond 100 MeV.[17,18]

The two clusters of particles travel toward a converter where the charged particles are decelerated, generating hard x rays (1–10 MeV), which, in turn, may produce some photoneutrons if appropriate target material is available (e.g., tungsten). Deuterons with energies of 1–10 MeV may produce neutrons by nuclear reactions, such as deuteron break-up,[19,20] preserving the momentum of the deuterons and therefore producing a neutron pulse predominantly traveling in the direction of the initial laser pulse.[21,22] A material with suitable cross sections for deuteron break-up is beryllium.

As mentioned, the configuration of the primary target for the laser and the secondary target or "converter" for the accelerated particles is called pitcher–catcher configuration. A challenge arises in providing suitable target material of the correct thickness at repetition rates of 1–100 Hz, which is a current field of research and a main inhibitor for deploying a laser-driven neutron source capable of delivering neutron pulses at repetition rates suitable for applications. The target thickness of the pitcher target needs to be controlled to better than 100 nm and must match the laser parameters; otherwise, orders of magnitude fewer neutrons than

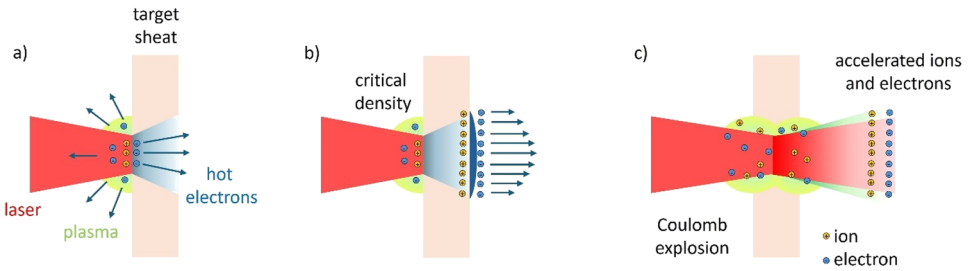

FIG. 1. The process of laser-driven ion acceleration. A laser pulse impinges on a target sheath and creates a plasma (a). A fraction of the laser energy is transferred to the electrons, which create a sheath at the rear target surface (b). This charge separation creates a strong electric field that is capable of accelerating ions from the surface. If the target is thin enough, the laser can propagate through the target and enhance the acceleration (c). [Reproduced and adapted with permission from M. Zimmer, "Laser-driven neutron sources–A compact approach to non-destructive material analysis," Ph.D. dissertation (Technische Universität Darmstadt, 2020). Copyright 2020 Author(s), licensed under a Creative Commons Attribution 4.0 license.]

with proper thickness are produced. Secondary effects, such as the so-called breakout-afterburner process, predicted in theory[23] and demonstrated experimentally,[24] may further enhance the neutron yield by up to an order of magnitude. During the break-out afterburner process, after electrons are already swept out of the target material, the still ongoing coherent photons of the laser pulse cause the remaining electrons to oscillate in their field, making them relativistically heavy. This, in turn, makes the remaining target material transparent as the attenuation by "light" photons is reduced, which allows us to further improve the interaction of the laser pulse with the target material to accelerate particles to up to an order of magnitude higher energies to increase the cross section for the subsequent neutron production. For such processes, the laser pulse shape and target geometry need to be extremely well controlled. Laser yields up to 10^{10} neutrons per pulse were achieved with such methods.[21,22]

For the purpose of efficient laser-driven neutron generation, continuously flowing (high-velocity >100 m/s) cryogenic jets are ideal high-repetition sources for proton or deuterium beams.[25] The small size of the refreshing target allows for controlled *in situ* density tailoring enabling proton beams with energies up to 80 MeV from repetitive ultra-short pulse petawatt lasers.[26] Recently, a high-repetition-rate compatible platform was presented using a pitcher–catcher setup with a planar cryogenic liquid deuterium jet (pitcher) and an adaptable converter (lithium and/or beryllium) to generate high-flux directed neutron beams at high repetition rates.[27] The combination of a high-pulse-rate laser with the quickly replenishing target allows for operation at rates up to 1 kHz in principle.

2. Laser wakefield acceleration (LWFA)

An alternative method for realizing LDNS involves laser wakefield acceleration (LWFA). LWFA utilizes the interaction between intense laser pulses and a plasma to accelerate electrons to high energies.[28] In LWFA, a high-intensity laser pulse is focused onto a gas, typically a combination of hydrogen or helium and nitrogen or oxygen.[29] Upon interaction, the laser ionizes the gas, creating a plasma and driving a non-linear plasma wave, which is trailed by a wakefield. Electrons can become trapped in this wakefield and thus be accelerated to relativistic energies, forming an energetic electron bunch that travels along the path of the laser pulse. The mechanism of LWFA relies on the ponderomotive force induced by intense laser fields, which displaces electrons in the plasma from regions of high intensity to low intensity regions, creating large longitudinal electric fields. The characteristics of the generated electron bunches depend on various parameters, such as laser pulse intensity, duration, and the properties of the target plasma. Based on the combination of these factors, the resulting electron bunch can exhibit either a continuous energy distribution similar to TNSA or a narrow, quasi mono-energetic distribution with a full width at half maximum (FWHM) of around 25% or less of the peak central energy.[30,31] Recent advancements in LWFA technology have led to the routine achievement of electron energies exceeding 100 MeV, with reported maximum energies reaching up to 8 GeV.[32,33] Moreover, LWFA electron beams can exhibit low divergence in the range of several milliradians, making them highly collimated and suitable for various applications. In simulations, electron to neutron conversion efficiencies up to 25% have been shown with laser-accelerated electron bunches, resulting in theoretical neutron currents of 10^7–10^8 n/pulse.[34] LWFA therefore has the potential to mitigate some of the problems with solid targets discussed below.

One of the key advantages of LWFA for LDNS is its scalability and compatibility with laboratory scale setups. By utilizing lower energy laser systems (e.g., at or above 100 mJ class), efficient electron acceleration and subsequent neutron generation can be achieved.[35–38] This scalability opens doors for smaller research facilities to access neutron sources, which were traditionally limited to larger, more expensive setups. Furthermore, LWFA-LDNSs offer the potential for high repetition rates, enabling the production of neutron pulses at kHz-level frequencies.

C. Target system

For a TNSA based laser-driven neutron source, the target has to be thin enough to benefit from the effects of relativistic induced transparency, should be available or produced in large quantities, and has to be stably operated at a high repetition rate, such as 10–100 Hz for thermal/epithermal neutron applications or 1–100 kHz for MeV neutron applications. Besides that, it needs to be large enough to be reliably hit by the laser, and the target system has to survive the laser impact. For high repetition rates, it is also important that the target is mostly debris free to avoid deterioration of the laser optics in the target chamber. Additionally, an operation with protons as well as with deuterons should be possible.[39]

State-of-the-art target technology for current TNSA LDNS is deuterated polymer foils in the sub-μm regime. These targets are produced by dissolving deuterated polystyrene in butanol and applying it via spin-coating to a flat silicon wafer. With a variation in rotation frequency and polymer concentration in the solution, the thickness can be tuned. Although there are many advantages to this type of target, there are also downsides to this technology. For example, solid plastic targets produce more debris than liquid targets, and the debris is often in the form of molten polystyrene, which coats nearby optics and parts of the final focusing parabola. This reduces the performance over time. Overcoming the limit of matrix targets, it is possible to utilize a VHS tape for a TNSA target. Since the tape is not deuterated, mostly protons and carbon ions are accelerated with these targets.

Another option is to use a continuous, micrometer-sized cryogenic cylindrical or planar liquid jet as a laser target. The jets exhibit a high laminarity and stability for centimeters and can theoretically operate without interruption as long as they have a sufficient supply of processing gas (target material) and liquid helium as coolant. They allow for the generation of single species particle beams, determined by the choice of gas for target production. Apart from hydrogen as a source of pure proton beams, other gases such as deuterium, helium, argon, or neon can be used to deliver a continuous jet as a self-refreshing and debris-free target.[40] For neutron generation, deuterium jets provide a pure D^+ beam without the contamination of protons that otherwise reduce the acceleration efficiency in solid deuterated foil targets. The operation of such systems in the harsh environmental conditions of high-power laser induced plasma experiments has turned out to be challenging. Damage to the jet target system during application of full energy laser pulses has been prevented by the implementation of a mechanical chopper system interrupting the direct line of sight between the laser plasma interaction zone and the jet source.[41] It is also possible to operate

liquid jets or synchronized droplets with water or ethylene glycol at room temperatures, including deuterated target materials. This enables a significantly higher hit rate as well as an increased pulse to pulse reproducibility due to less influence of the laser pointing stability.

However, target systems for electron-based LDNS are completely different. To achieve efficient laser wakefield acceleration (LWFA), gas targets are used as a medium in which the high-intensity laser generates the necessary plasma.[4] These gas targets come in various forms, including supersonic gas jets, gas cells, or capillary discharge waveguides, each tailored to specific experimental requirements and target parameters.[33,38,42–44] By injecting gases such as a combination of hydrogen or helium and nitrogen or oxygen, among others,[29] into the path of the laser and adjusting gas pressure during injection, researchers can control plasma density, influencing electron acceleration and beam divergence. Gas jet or nozzle targets, in particular, offer precise control over plasma density gradients, crucial for enhancing beam quality and stability.[38,42–45] Moreover, the choice of gas target influences the injection mechanism of electrons into the wakefield, with options ranging from ionization injection to density ramping or colliding pulse injection, each impacting the resulting electron beam properties.[32]

One significant advantage of gas-based targets over TNSA targets is their inherent compatibility with high repetition rates and low debris generation. With laser energies exceeding 1 J, stable operation at frequencies up to 1 Hz over extensive pulse counts of over 100 000 pulses has been demonstrated using gas targets.[46] Furthermore, advancements in LWFA have enabled operation at kHz-level repetition rates, even at lower laser energies around 10 mJ, highlighting the versatility and scalability of gas targets for LDNS applications.[47,48] The stability and reliability of gas targets make them ideal candidates for long-duration experiments.

D. Technical requirements

TNSA based LDNSs operate by accelerating protons and deuterons through the interaction of high-intensity laser irradiation (intensities exceeding 10^{18} W/cm^2) with sub-micrometer-thick targets. These accelerated ions are subsequently directed onto a "catcher" material, which initiates neutron emission via nuclear processes (see Fig. 2). Charged particles in a LDNS with a pitcher–catcher configuration only travel distances of centimeters rather than a few meters as in compact accelerator-based neutron sources or even hundreds of meters as in spallation neutron sources. This removes the need for magnets to keep charged particles together, a considerable part of the investment and energy consumption of accelerator-driven sources. The duration of the entire neutron generation process is less than a nanosecond, enabling inherently short neutron pulses requiring otherwise investment into proton storage rings to achieve pulse lengths of hundreds of nanoseconds at spallation sources, while compact accelerator-driven neutron sources are limited to initial neutron pulse lengths of tens of microseconds. This makes LDNSs, in particular, useful for neutron techniques requiring time-of-flight techniques.

Utilizing this approach, LDNSs have demonstrated the generation of neutrons spanning initial energies ranging from 100 keV to as high as 100 MeV. Recent experimental endeavors have showcased the achievement of short neutron pulses, yielding up to 10^{10} n/s, with pulse durations of less than 1 ns. Requirements and problems of such systems are as follows:

- Reliable lasers with sufficient:
  - Energy: 10–1000 J to achieve neutron production rates of at least 10^{10} n/s for meaningful neutron measurements with the repetition rates discussed below.
  - Pulse duration: fs to ps pulses. Too long pulse durations lead to reduced efficiency of the ion acceleration process and hence a decreased neutron production.
  - Focus: minimal focus spot size of down to 1.35 μm (FWHM),[49] limited by diffraction of the laser pulse with itself. This puts demand on the lenses and deformable mirrors.
  - Contrast: amplified spontaneous emission or prepulses should not cause ionization or, in the worst case, destroy the target (not exceeding ~10^{13} W/cm^2).
  - Repetition rate: 1–100 Hz for thermal/epi-thermal neutrons, higher rates applicable for MeV neutron time-of-flight applications. Repetition rates below 1 Hz are only useful for proof of principle experiments, while repetition rates above 100 Hz are not compatible with thermal/epi-thermal neutron flight times due to pulse overlap.

- Pitcher systems with appropriate:
  - Thickness: target thickness needs to be suitable for the laser parameters, in particular, laser contrast and intensity. Mismatch of target thickness and laser parameters by tens of nm can decrease neutron production by orders of magnitude.
  - Target Area: lateral dimensions of the target need to exceed the laser spot size (several μm).
  - Material Composition: light elements (preferably hydrogen nuclei) are required for efficient acceleration and neutron production.
  - Target position along the laser direction: position needs to be reproducible in the focal spot of the laser as any deviation greatly decreases the production efficiency due to decreased intensity on target.

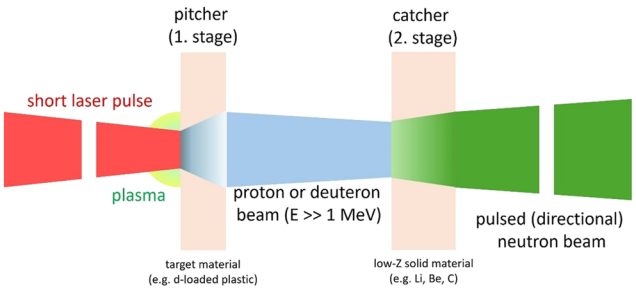

FIG. 2. Schematic of a laser-driven neutron source utilizing pitcher–catcher configuration. [Reproduced and adapted with permission from Vogel *et al.*, EPJ Web Conf. **231**, 01008 (2020). Copyright 2020 Author(s), licensed under a Creative Commons Attribution 4.0 license.]

- Debris: the target should not produce substantial debris contaminating optical components in the target chamber.
- Repetition: providing suitable targets fulfilling the aforementioned criteria at the necessary repetition rates has proven to be a substantial technical problem. Some approaches to solve this problem are discussed below.

- Catcher system:
  - Neutron yield: the material needs to be chosen depending on the neutron production cross sections for the given ion type and energy.
  - Chemical hazards: typical catcher materials, such as beryllium or lithium, may pose handling hazards requiring special safety measures, such as providing the material as a compound rather than pure.
  - Radiological hazards: target materials such as tungsten or uranium may activate during operation.
  - Operational hazards: efficient target cooling to avoid thermal destruction of the target, avoidance of blistering, and avoidance of debris during operation.
    -Avoidance of blistering is challenging due to the broad energy spectrum of the particle beam, which hampers established solutions.

In newer laser systems, advancements in laser diode pumping and the incorporation of active cooling systems have enabled significantly improved heat removal efficiency. As a result, these systems exhibit substantially elevated repetition rates. For instance, the Extreme Light Infrastructure (ELI) L3 beamline[50] is poised to operate at 1 PW with a pulse duration of 30 fs and an energy of 30 J, maintaining a repetition rate of 10 Hz. Similarly, the proposed Scalable High-power Advanced Radiographic Capability (SHARC) laser system at the Lawrence Livermore National Laboratory (LLNL) is projected to deliver 150 J over a pulse duration of 150 fs at a repetition rate of 10 Hz.[51] In this configuration, neutron current exceeding 5×10^{11} n/s is anticipated, affording a neutron flux suitable for relevant applications.

For this LDNS type, a debris free target is required to prevent a degradation of the optics over time, reducing the neutron production. The target also needs to be self-renewing at a rate faster than the laser repetition rate to ensure an undisturbed and stable target present once the laser hits the target. Morrison *et al.*[52] demonstrated that a liquid leaf target theoretically can fulfill these conditions for laser ion acceleration up to the kHz range, even though with limited pulse energies of 5 mJ, which resulted in a 70 μs recovery time. Treffert *et al.* used a similar liquid leaf with up to 5.5 J at the ALEPH laser to accelerate protons 3.5 MeV and deuterons up to 1.9 MeV per nucleon with a repetition rate of 0.5 Hz.[27] Experiments of the TU Darmstadt have reached over 16 MeV using a liquid leaf at the Vega 3 system, but results have not been published yet.

Using intense heavy ion beams, a compact neutron generator source has been proposed based on the kinematic focusing technique and direct plasma injection scheme.[53] Here, a dense and highly ionized plasma (e.g., $^7Li^{3+}$) is produced by a laser ablation. The plasma expands to a radio-frequency quadrupole (RFQ) linac and the ions are extracted at the entrance. Then, the ions are bunched and accelerated and guided to a proton containing beam target to release neutrons. With a proposed repetition rate of 100 Hz and a pulse width of 10 μs, an average neutron flux from the target of 10^9 n/cm^2/s has been predicted.[53] The proposed compact neutron generator could be applied in many fields, for example, nuclear data measurement, non-destructive inspection for security, the defect detection of buildings, isotope production, or fast neutron therapy.

E. Neutron moderation

As the binding energy of neutrons in the nucleus is commonly a few MeV, free neutrons usually have initial energies in the MeV-regime. Except of fast (MeV) neutron imaging techniques, classical neutron scattering and spectroscopic methods require much lower energies in the range of a few eV down to meV or below (thermal and cold neutron). To decrease the energy by more than 6–9 orders of magnitude, moderators are used.[4] A benefit of LDNS with respect to moderation is the generation of neutrons predominantly in the direction of the laser pulse, which may enable improved target/moderator coupling compared to, for example, spallation sources. While proof of principle LDNSs producing thermal neutrons typically used solid plastic as a moderator, even with the catcher target embedded, to the best of our knowledge, no full design of target, target chamber, and moderator optimized for this specific source type has been reported.

The lighter the nuclei of the scattering material are, the higher is the amount of energy transferred in every collision. For that reason, materials with a high total scattering cross-section, such as hydrogen, beryllium, or carbon, are preferable for neutron moderation. Although a fast slowing down is desirable, a good moderator also has to have a low neutron absorption cross section Σ_a to keep the yield of cold and thermal neutrons from the moderator high.

In Table I, several common moderator materials are compared, showing the moderation (slowing down) power and the moderating ratio, which is the ratio of the slowing down power and the absorption cross section.

TABLE I. Parameters for different moderation materials. An efficient moderator needs to have a high moderation power and a high moderation ratio to minimize the moderation time t_{mod}. n_{mod} is the average number of collisions to thermalize and t_{diff} is the diffusion time before neutrons are absorbed. [Reproduced and adapted with permission from M. Zimmer, "Laser-driven neutron sources–A compact approach to non-destructive material analysis," Ph.D. dissertation (Technische Universität Darmstadt, 2020). Copyright 2020 Author(s), licensed under a Creative Commons Attribution 4.0 license.]

Material	Moderating power $\xi\Sigma_{el}$	Moderating ratio $\xi\Sigma_{el}/\Sigma_{abs}$	t_{mod} (μs)	n_{mod}	t_{diff} (s)
Water	1.36	62	10	20	2×10^{-4}
Heavy water	0.18	5000	46	27	2×10^{-1}
Beryllium	0.16	145	67	86	4×10^{-3}
Graphite	0.06	165	150	114	1×10^{-2}
Polyethylene	3.26	122	5–10	20	1×10^{-4}

In the case of laser neutron sources or accelerator-driven sources, a solid moderator is preferred as it has a higher compatibility with the required vacuum systems. Based on efficient moderator coupling of a LDNS, the pitcher–catcher configuration could deliver a higher fraction of neutrons moderated for experiments.

F. Shielding and infrastructure requirements

Laser-based neutron sources offer the possibility of developing compact beamlines, closely coupled to the moderator, thanks to the significantly less hostile environment offered by a laser-based system compared to reactor and spallation neutron facilities but comparable to CANS and HiCANS.[4]

For spallation sources, the neutrons produced by the intranuclear cascade process reach energies up to the proton energy (e.g., ~1 GeV). While the fraction of neutrons with those highest energies is small, however, the shielding demands are driven by this small fraction of neutrons released with the highest energies. Modern spallation sources therefore have their closest sample position outside the bulk shield at about 15–20 m, e.g., the high-pressure beamline SNAP at the SNS has a moderator to sample distance of ~15 m.[54] At LANSCE, a neutron source about an order of magnitude less powerful than the SNS, the bulk shield ends at 4.5 m with the closest possible sample position that allows some collimation being around 6 m. Similar distances are present at reactor-based sources. Flux on sample, a main driver for count time requirements, scales with $1/L^2$ unless beam guides for cold and thermal neutrons can be used. Volume of target and beam path shielding is a considerable cost factor for a neutron source.

In comparison, laser-driven neutron sources require significantly less shielding of ~1 m, which allows compact and efficient placement of neutron optical systems and saves significant cost spent on necessary radiation protection measures. In this respect, laser-driven neutron sources are similar to the accelerator-driven sources with low ion energy, the so-called CANS and HiCANS facilities. For such sources, requirements on space, infrastructure, and power are far less in comparison to, for example, accelerator based spallation neutron sources (e.g., SNS, J-PARC, and ESS[4,55]).

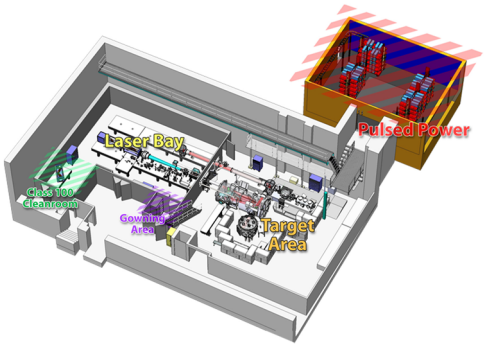

FIG. 3. The Texas Petawatt laser facility, which occupies a clean room area of 140 m^2 for the laser system and a total floor space of about 600 m^2[57] (Public domain image, courtesy of The University of Texas at Austin. Source: https://texaspetawatt.ph.utexas.edu/facility-layout.php).

III. CURRENT STATE AND APPLICATIONS OF LASER-DRIVEN NEUTRON SOURCES

A. Examples of laser-driven neutron sources and installations

Laser-driven neutron generation was demonstrated at several facilities, typically with pitcher–catcher configurations, and the production of 10^{10} neutrons per pulse with 70 J lasers has therefore been reproduced at different facilities. Those facilities include the TRIDENT laser at the Los Alamos National Laboratory,[56] the Texas Petawatt Laser at the University of Texas in Austin (Fig. 3),[57] the PHELIX laser at the Gesellschaft für Schwerionenforschung in Darmstadt,[58] the VULCAN laser at AWE in the U.K.,[59] and others. These lasers can produce single pulses and do not operate at repetition rates suitable for data collection for some 100–1000 pulses or so. Lasers with a repetition rate of 1 Hz or more, such as the DRACO laser in Dresden,[60] the BELLA laser at Lawrence Berkeley

TABLE II. Basic parameters of current laser facilities with reported or estimated neutron production.

Source	Neutron production rate (n/pulse)	Laser energy (J)	Repetition rate (Hz)	Laser pulse duration
TRIDENT LANL[21,56,63]	5×10^9	80	NA	~600 fs
Texas Petawatt Laser[57,64]	1.6×10^7	180	NA	170 fs
PHELIX GSI[58,65]	$\sim 10^{11}$	120	NA	0.4–20 ps
VULCAN RAL[59,66]	$\sim 10^7$	~400	NA	~500 fs
DRACO HZDR[60,67,68]	$\sim 10^9$	30	NA	30 fs
Apollon LULI[68]	$\sim 10^8$	40	NA	24 fs
BELLA LBL[61,66,69]	$\sim 10^{10}$	30–40	1 Hz	50–200 fs
ALLS INRS[70]	5×10^5	3	0.5 Hz	22 fs
ALEPH CSU[27,62,71]	7.2×10^9	5.5	0.5 Hz	45 fs
ELI ALPS[72,73]	2.1×10^4	0.023	10 Hz	12 fs
SHARC LLNL[74]		150	10 Hz	150 fs
LFEX UOsaka[75]	$\sim 10^{11}$	~1000	NA	1.5 ps

Laboratory,[61] or the ALEPH laser at Colorado State University,[62] provide at least an order of magnitude less laser energy. An overview of these laser facilities is given in Table II.

Target systems allowing neutron production at increased repetition rate were demonstrated at such laser systems[25,76] and can be deployed once lasers providing 100 J or more at repetition rates of 1 Hz or more are available. However, no laser has been designed specifically for the purpose of ion acceleration to enable neutron and x-ray production for material characterization. The aforementioned laser systems are all designed and operated as multi-purpose laser user facilities, in the United States accessible through LaserNET,[77] but serve many more purposes than particle acceleration for neutron or x-ray production. Therefore, each time beam time is awarded to develop, for example, laser-driven neutron sources, target chambers have to be re-configured, requiring laborious alignment and installation of control electronics into vacuum chambers, etc.

B. Applications

Neutron pulses from a laser-driven neutron source are extremely short <1 ns[78] compared to conventional neutron pulses from spallation sources with proton storage rings (e.g., 270 ns at LANSCE, 700 ns at SNS, 3 ms at ESS) and conventional compact neutron sources, such as the RIKEN Accelerator-driven Compact Neutron Systems (RANS) source (>8 μs).[79–81] The FRANZ project proposes a high intensity short micro-bunch of 1 ns for neutron capture cross-section measurements.[82] Given the moderation time (as measured by the neutron pulse width emitted from the moderator) of, for example, >20 μs for thermal (<0.4 eV) and 1 μs for epithermal neutrons (10 eV, shorter with increasing neutron energy)[83] and the requirement that the neutron pulse length must be negligible compared to the moderation time to avoid the neutron pulse length to contribute to the instrument resolution, laser-driven neutron sources are best suited for time-of-flight methods. Above 1 eV, LDNSs can achieve higher energy resolutions compared to spallation sources due to their short pulse width.[84,85]

An overview of requirements on neutron source current and application parameters is given in Table III.

1. Imaging/radiography

Applications of neutron radiography span the market of non-destructive testing, for example, aerospace, aircraft and military components, turbine blades, and welding. Commercial as well as public institutions offer such services.[86,87] LDNSs can be used for safety and performance assessment for critical components, detecting defects, and ensuring optimal functionality. As a potentially mobile device, it can be used for bridge inspection, identifying weaknesses by detecting faults in the structural components while at the same time identifying the corrosion level inside the bridge material via prompt gamma neutron activation analysis (PGNAA).[88] In hydrogen fuel cells and battery technology, neutron radiography can be used to identify internal processes during operation to monitor local hydrogen production or the formation of dendrites. This improves R&D speed as well as the component lifespan. For prototype inspection, 3D printed objects are prone to have defects from the manufacturing process. Neutron radiography and tomography can be used to identify internal defects, voids, or incomplete fusion of metal parts. Fast neutron imaging and PGNAA using LDNS can be used to non-destructively identify the content of shielded

TABLE III. General neutron applications and required neutron energies, resolution, and source current (or source strength).

Application	Neutron energy range	Energy resolution	Neutron source current
Imaging (not white beam)			
- Radiography, tomography	0.01 eV < E < 1 keV	<2%	
- Bragg-edge imaging,	0.1 eV < E < 0.5 keV	<1%	10^{10-11} n/s
resonance imaging	1 eV < E < 1 keV	5%	
Medical applications			
- Boron neutron capture therapy	0.1 eV < E < 1 keV		
- Tissue irradiation	0.1 eV < E < 1 keV	None	10^{12-13} n/s
- Isotope production	0.1 eV < E < 1 keV		
Irradiation			
- Single event effects	1–30 MeV		
- Silicon doping	<10 keV	None	10^{14-15} n/s
- Activation analysis	1 eV < E < 1 keV		
Material processing and scattering			
- Stress and strain measurements,	<0.1 eV	<0.3%, <1%	
phase analysis	<0.01 eV		
- SANS	0.01 eV < E < 0.2 eV	10%	
- Diffraction	0.001 eV < E < 0.03 eV	<0.1%, <10%	$\geq 10^{14-15}$ n/s
- Neutron spectroscopy	1 eV < E < 10 keV	<1%	
- Resonance spectroscopy	1 eV < E < 10 keV	<0.3%	
- Activation analysis (PGAA)	1 eV < E < 1 keV	<0.3%	

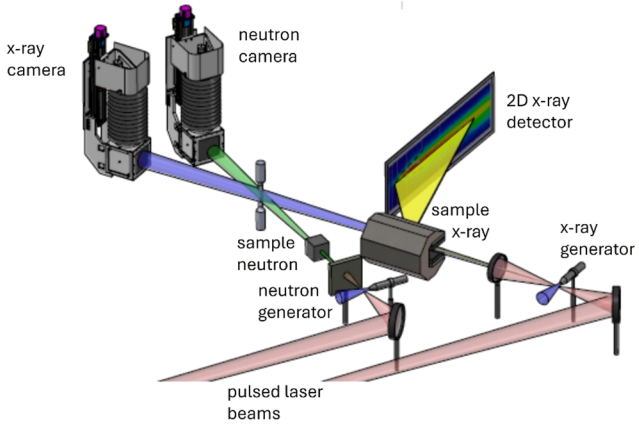

FIG. 4. A proposed configuration (not to scale) for a laser-based combined x-ray/neutron imaging facility. The facility is configured for a 100 Hz, 25 fs, 1 J/pulse laser with a mirror system that will feed either the x-ray generator or the neutron generator for concurrent x-ray and neutron imaging. The footprint of the imaging facility is estimated to be 2×3 m^2.

nuclear waste drums.[89] As these types of containers are shielded against gamma radiation, standard x-ray radiography is ineffective. Neutron radiography can penetrate the lead shielding and provide information about the internal content.

For imaging applications, laser-driven neutron and x-ray sources provide unusually small, nearly point-like source sizes, enabling divergent cone beam imaging or magnification geometries providing superior spatial resolution. This is due to the small laser spot size (~μm) generating a small cloud of accelerated particles on the order of 10 μm that are ultimately converted to neutrons or x rays. For neutrons, this spatial resolution is, of course, only true for unmoderated MeV neutrons.[63] Once moderated, the origin and size of the neutron source are, besides the neutron pulse structure, indistinguishable, whether it is a reactor, spallation, DD generator, or laser-driven neutron source. The sketch shown in Fig. 4 is configured for a 100 Hz, 25 fs, 1 J/pulse laser with a mirror system that will feed either the x-ray generator or the neutron generator for concurrent x-ray and neutron imaging. An operational goal is stroboscopic imaging with a high temporal resolution x-ray imaging, simultaneously supported by cold neutron imaging. The anticipated results would allow the detection of crack opening and closing during the load cycle and then the correlation of the crack activity with hydrogen concentration. An unresolved parameter is the time structure of the two laser beams. The default time structure is not simultaneous but rather beam switching between the two paths with a frequency of 0.01 Hz or slower.

Radiography with laser-driven sources implemented with both thermal neutrons and x rays was reported in Refs. 90 and 91. Laser-driven x-ray radiographies have been performed by Refs. 22 and 92. Comparable experiments using a single LDNS pulse for neutron radiography were shown in Refs. 22 and 84. Radiography images were obtained with a single pulse of the LDNS, while most radiography studies took data from multiple pulses to obtain an integrated radiography image. Recently, a concept for a multimodal x-ray/neutron imaging platform at single pulse and high repetition rate was presented.[93] Considering the features of short pulses of LDNS, it is promising that a "snapshot" for the investigation of high-speed phenomena inside matter can be achieved via using a laser-triggered radiography system. Using a Be cube as a neutron generator and a stack of CR-39 solid trackers in the radiography shot to record the number of fast neutrons,[90,94] radiographs of a nickel–cadmium (Ni–Cd) battery, a nickel-metal hydride (Ni-MH) Cd-free battery, and a boron carbide (B_4C) powder were obtained. The results highlight the advantage that neutrons have in diagnosing materials that cannot be recognized by x rays.[95]

Furthermore, short-pulse sources enable diffraction-contrast imaging[96] utilizing the so-called Bragg-edges,[97] which can be used to, for example, map in 2D and by tomographic methods also in 3D the phase fractions[98] or strains[99] present in a sample. Combined with resonance methods, which can be conducted simultaneously, this allows for unique and hitherto rarely applied characterization capabilities.[100] A proof-of-concept of neutron resonance imaging with lasers was applied to identify cadmium in a sample arrangement by scanning through resonant and non-resonant energy ranges.[84] If constant wave (CW) or longer pulse sources are required, e.g., for white beam neutron radiography, DD or DT neutron generator sources provide reasonable neutron fluxes and are established technologies.

Utilizing short neutron pulses moderated into the epithermal neutron energy regime for imaging applications, epithermal neutron imaging, for example, can be applied to identify and map isotopes[101,102] and quantify their density.[103,104] Despite the challenge to detect fast neutrons because of their low cross sections, detection efficiencies above 25% (2 MeV neutron energy) can be achieved.[89,105,106] Due to the small source sizes in the order of millimeters, LDNS could provide a high spatial image resolution.

Fast and epithermal neutrons can also play a crucial role in the evaluation of the structural integrity and the isotope distribution of activated materials, e.g., fuel rods in nuclear reactors. They can be used to non-invasively inspect meter-sized closed waste containers or cargo and detect light materials, such as residual water or explosives, even behind heavy shielding.[89]

2. Nuclear physics and astrophysics/nuclear cross-section measurements

Cross-sections measurements[107] require neutrons in the epithermal neutron energy range (0.4 eV to 100 keV). While still requiring moderation, these measurements benefit, in particular, from the sub-nanosecond pulse length of the initial neutron pulse prior to moderation. Besides neutron absorption-based neutron radiography, such measurements would benefit from a laser-driven neutron source if neutron fluxes are surpassing, e.g., the flux of 3.4×10^{13} n/s in 10 ns long pulses at 800 Hz at the electron-driven GELINA facility.[108]

The neutron energy spectrum also plays a key role in nuclear astrophysical experiments. The neutron energy spectra obtained with those configurations have peaks around 1 MeV. Depending on what nuclear astrophysical process one wants to study, the energy of the particles at play can vary considerably. The temperature at which the r-process is estimated to happen is around 1.2 GK. If we assume a Maxwell–Boltzmann distribution, it gives a mean energy

of 100 keV, which is not so far from the peak energy obtained by Martinez *et al.*[109]

High-flux, short-pulse neutrons would make possible the direct measurements of neutron capture and β-decay rates related to the r-process of nucleosynthesis of heavy elements. They would also allow for nuclear measurements in a hot plasma environment, which would be beneficial for s-process investigations in astrophysically relevant conditions. This could, in turn, finally allow possible reconciliation of the observed element abundances in stars and those derived from simulations, which at present show large discrepancies.[110]

3. Neutron resonance spectroscopy

High-energy neutrons are necessary to be moderated for applications where epithermal or thermal energies are preferable. One of these is neutron resonance spectroscopy (NRS), which, among others, allows us to identify the elemental and isotopic composition of bulk materials that have pronounced resonances in this energy regime.[104,111] In NRS, the attenuation of neutrons through a sample is measured using the time-of-flight of a short-pulsed neutron source. Absorption resonance Doppler-broadening to map a bulk temperature[95] or the quantification of the density of gas nuclei to measure the gas pressure were also performed at the accelerator-driven neutron sources.[102]

Higginson *et al.* proposed the feasibility of laser-driven NRS for temperature measurements by Doppler broadening of neutron absorption resonances with a neutron yield of 1.8×10^9 neutrons in a picosecond pulse on the condition that the moderator has to slow down fast neutrons and direct them toward the sample.[112] Fernandez *et al.* laid out the requirements of a LDNS to measure the bulk temperature of a sample with a single neutron pulse, for example, during a shock experiment probed with other means, such as an x-ray free electron laser.[113,114]

With the efficient generation of epithermal (0.1–100 eV) neutrons, single-shot analysis of composite materials by neutron resonance transmission analysis (NRTA) has been demonstrated for the first time[115] with a LDNS at a time-of-flight distance of 1.78 m with sufficient energy resolution for element identification. The laser-driven NRS setup has been utilized to demonstrate a transparent temperature measurement of a metal sample from the Doppler broadening of the resonance signal.[116]

4. Neutron activation analysis

Neutron activation analysis (NAA) is a non-destructive method to determine the isotopic composition of materials based on the neutron capture or (n, γ) reaction. There are two categories of NAA: the direct gamma de-excitation right after the neutron capture or prompt gamma neutron activation analysis (PGNAA) and the radioactive decay of the unstable nuclei afterward or delayed neutron activation analysis (DNAA).[117] NAA is used in a wide range of applications in industry, such as mining, concrete production, and nuclear waste, in agriculture to identify trace elements in soil, or in cultural heritage for non-destructive chemical analysis of artifacts. With a short-pulse neutron source, the neutron time-of-flight may allow us to identify the energy of the captured neutrons, which, in conjunction with the energy of the emitted gammas, may allow us to identify the absorbing nucleus.[118] In the decay phase, short-lived decay lines might be collected with acceptable counting statistics on an extremely low baseline.[119] For delayed neutron activation analysis, laser-driven neutron sources do not provide the significant benefit of CW sources.

5. Radiation/irradiation

Particle interactions can lead to destructive interactions in the material. The displacement damage reaction is a nuclear process that results in the displacement of a lattice atom, leaving a hole or defect in the formation, that initializes various other effects that alter the properties of the material.[120]

With the prospect of a demonstration of a nuclear fusion reactor within the next 20 years, it is imperative to study the effects of neutron bombardment on the materials that will be used for these devices.

An increasing concern is single event effects (SEEs) in modern semiconductor technologies as devices are designed to be as small as possible.[121,122] In particular, semiconductors such as chips and SRAMs, used in flight operations on Earth and in space, receive neutron radiation.[123] Neutron fluxes in the range from 10^4 to 10^9 n cm^{-2} s^{-1} at neutron energies of 1–4 MeV are of interest to investigate SEEs on components. With the introduction of LDNS, a new solution arises for SEE tests.

High-repetition-rate laser-driven neutrons also provide opportunities for radiobiological investigations using a neutron beam with unique characteristics, such as short bunch duration and high dose rate. Recently, experiments with zebrafish embryos and glioblastoma human cell lines were performed at the ELI ALPS laser-based neutron source.[72]

Another aspect is the production of medical radioisotopes by neutron capture for diagnostic and therapeutic applications.[6] Alternative routes for the production of radioisotopes as ^{99m}Tc or ^{177}Lu is of general interest to stabilize the resilient production of these medical isotopes when nuclear reactors are not available.[124] There may also be the advantage of producing the radioisotopes closer to the hospital using many decentralized LDNS, as the distance to the production site is a problem for short lived isotopes.

6. Small angle neutron scattering

Scattering applications, besides neutron imaging, are likely the most desirable for end users (Table III) Since there are countless neutron scattering techniques that could be implemented we discuss here as an example for neutron scattering applications to a first generation laser-based neutron source, a possible design of a pulsed SANS beamline similar to the compact SANS currently under construction at LSU[125] has been proposed.

To mitigate the reduced source intensity per pulse, the source repetition frequency can be increased, leading to either a short baseline pulsed setup or above roughly 200 Hz to a SANS beamline whose characteristics are practically continuous. For a 200 Hz source frequency, a very compact SANS setup with about 2 m distance between the moderator and detector allows a neutron band width of 1–10 Å and together with a 0.5 m diameter detector, resulting in about two orders of magnitude in Q-range (about 0.01–1 Å^{-1}). For the first-generation laser-based SANS setup, the resolution and Q-range of the instrument must likely be reduced in favor of more

intensity, aiming for a measurement duration of 24 h or less per sample. For weakly ordered materials, the data point density and statistical certainty per point in the analysis can be reduced, reducing the required measurement time by several orders of magnitude. Together, these measures will limit the range and resolution of the SANS experiments as well as classes of samples to be measured in such an instrument, but measurements within a day are possible.

Figure 5 shows the output of simulations of SANS intensities with realistic resolution functions for (i) a conventional high-performance pinhole SANS instrument (with $\Delta Q/Q = 5\%$) and (ii) a compact first-generation laser-based SANS using slit collimation (with 1 $Å^{-1}$ slit resolution height and 5×10^{-3} $Å^{-1}$ width). Here, perfect spheres and featureless fractals were chosen as demonstration objects. The lines in the graph represent spheres of different radii.

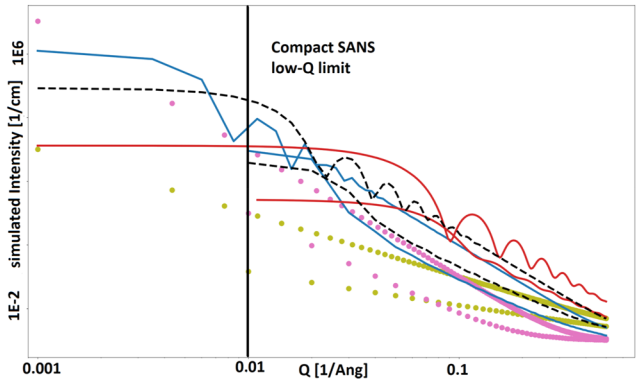

FIG. 5. Simulated SANS intensities of objects of different shapes: perfect spheres (lines) and fractals (dots). Each object was simulated at two setups: a conventional SANS setup with resolution $\Delta Q/Q = 5\%$ and a compact LDNS SANS setup with resolution with slit collimation (1 $Å^{-1}$ slit resolution height and 5×10^{-3} $Å^{-1}$ width) and low-Q limit $Q \geq 0.01$ $Å^{-1}$. Blue lines: 500 nm spheres, black dashes: 200 nm spheres, red lines: 50 nm spheres, violet dots: volume fractals, and olive dots: surface fractals. For the compact LDNS SANS setup, features in the simulated curves are diminished.

For each shape, two simulations are shown in the same color for the SANS geometries—for conventional high-performance SANS and compact LDNS SANS. The limited q-range ($Q \geq 0.01$ $Å^{-1}$) of the compact LDNS SANS design excludes the Guinier-regions of the scattering pattern for larger objects; hence, studies concerning the overall size of, for example, protein aggregates likely will not be possible in this setting. For smaller objects, such as nanomagnets or micelles, the Guinier-region is covered by both designs, and the overall size can be determined, but for the compact LDNS setup, features in the simulated curves are diminished. This is a result of the reduced point density in the simulations as well as the use of a slit-shaped optics. This is reversible, and a pinhole resolution could also be achieved in compact LDNS geometries.[126] Taken together, the simulated data show that it will likely be preferred to use instruments with higher intensity, higher resolution, and wider Q-range, but the simulations also demonstrate that for smaller nanoparticles and locally disordered and fractal samples, a first-generation laser-based SANS could be able to provide meaningful measurements.

C. Comparison with applications at reactor and spallation based sources

Spallation sources and pulsed nuclear reactors have the highest neutron yield in the order of 10^{15}–10^{18} n/s, which is several orders of magnitude higher than CANS and photofission sources (Table IV). Present day LDNSs have a comparably low neutron yield in the order of 10^{11}–10^{12} n/s, which is, however, still two to three orders of magnitude higher than portable neutron generators. If these numbers are compared to the actual thermal or epi-thermal flux at the detector position, these relations change drastically. Unlike for cold neutrons, current state-of-the-art neutron guides have limited benefits for thermal neutrons with a wavelength of less than 1 Å and show no benefit for epi-thermal neutrons. For this particular case, reactors might still have the highest average flux in the order of 10^9 n/cm^2/s at the detector, but this is measured without any energy resolution. Close to reactors, accelerator based HiCANS sources are expected to deliver comparable values. Spallation sources are left here at the highest detector flux rate of up to 10^9 n/cm^2/s thermal neutrons,

TABLE IV. Comparison of basic parameters between different neutron sources. [Reproduced and adapted with permission from M. Zimmer, "Laser-driven neutron sources–A compact approach to non-destructive material analysis," Ph.D. dissertation (Technische Universität Darmstadt, 2020). Copyright 2020 Author(s), licensed under a Creative Commons Attribution 4.0 license.]

Source	Neutron yield (n/s)	Thermal flux at detector (n_{th}/cm^2/s)	Min. Pulse length	Size (m)
Neutron tube	10^8–10^{10}	$<10^2$	5 μs	1
LDNS	5×10^{11}	$\sim 10^5$	< ns	15
Electron linac	3×10^{13}	$\sim 10^5$	1 ns	1–200
CANS	10^{13}	$\sim 10^5$	139 μs	10–50
HiCANS	10^{13}–10^{15}	$\sim 10^8$	1–1000 μs	30–100
Reactor	10^{16}–10^{18}	$\sim 10^9$	1–10 ms	10–30
Spallation	10^{15}–10^{18}	$\sim 10^9$	125 ns–625 μs	200–1000

which is several orders of magnitude higher than for LDNS as well as for CANS and electron linacs (Table III).[39]

The two orders of magnitude difference in detection and moderation efficiency between spallation sources and LDNS comes from two major factors. The neutron energies produced by laser acceleration are much lower. This reduces the absorption of neutrons inside the moderator material as well as the overall size of the moderator–reflector structure due to the compact source size. With a smaller moderator and a better energy resolution at an LDNS, neutron guide systems and detectors can be placed much closer to the source. A major limiting factor for applications is the pulse length. For all applications that rely on time-of-flight for energy differentiation, it is required that the flight time is large in comparison to the pulse length.

Comparing performances of different applications at different facilities has always been tricky and difficult because all sources, spallation sources, reactor sources, compact neutron sources, etc., are all to some degree unique. Even a comparison between only spallation sources is not really straightforward. At best, one could conclude that all the sources are more complementary rather than competitive. Nevertheless, to better understand what part of science laser-driven neutron sources could serve in the near future, an attempt is made to compare them to other neutron sources. The first question here is what metric one should use for that comparison. From a public/funding agent point of view, this metric should be related to the scientific output of the facility. While this is the ultimate metric, this kind of metric is extremely difficult and often very controversial to define. Going to the other extreme, one could use the brightness on the moderator surface as a performance metric. While this is much simpler, it ignores the fact that instrument designs are fundamentally different, e.g., a high-power spallation source, such as ESS,[127,128] and a source with a compact source target, such as the high brilliance source project HBS.[129] In case of ESS, the closest an instrument guide can be brought to the moderator source is 2 m, whereas in the case of the HBS, the guides are envisioned to be only a few tens of cm from the moderator surface. By bringing the guides that are closer to the moderator source, more useful neutrons can be captured and transported to the sample location. A compromise between these two options is the flux on the sample. While this metric does not account for items such as detector coverage, it does account for the neutron transport from the moderator to the sample location. There are also caveats in this case because one should compare instruments with the same resolution, Q-range, etc. Here, we will attempt to compare instruments that are as similar as possible. It has to be pointed out that the conclusions we attempt to draw for the laser-driven neutron sources will be based on an order of magnitude comparison but not more detailed.

Table V shows a comparison of fluxes on the sample position between HBS, ESS at 2 MW, and ILL for various instruments: small angle scattering, reflectometry, disordered material diffraction, cold chopper spectrometer, macromolecular diffraction, and imaging. It can be seen from the table that for most instruments at ILL and ESS, the flux on the sample is on the order of 10^7–10^9 n/cm^2/s, with the exceptions being the cold chopper spectrometers, which are on the order of 10^6 n/cm^2/s. However, one needs to keep in mind that the reduction of flux on the sample in the case of the cold chopper spectrometers does not come from differences in the source but from how these kinds of instruments work. Comparing these fluxes to the ones expected for the high brilliant source HBS,[129] it shows that the fluxes on the sample at HBS are between very competitive and about an order of magnitude below the high-power sources.

In case of the laser-driven neutron sources, the flux on samples that are currently feasible is on the order of 2×10^5 n/cm^2/s. While this is quite a difference, if one compares the laser-driven neutron sources to current university sources, instead of regional and international sources, the comparison becomes more favorable. In the case of the Low Energy Neutron Source (LENS)[131] at Indiana University, USA, the flux of the sample for the local SANS instrument is about 10^4 n/cm^2/s. This means that the currently expected fluxes for the laser-driven neutron sources are in the range of interest for universities or industry.

IV. TECHNICAL DEVELOPMENTS AND UPCOMING REQUIREMENTS

A. Development of laser sources

Laser technology to amplify and compress pulses has evolved dramatically since the first evidence of neutron production by lasers and at present. Strong magnetic and electric fields are accessible by intense laser pulses to enhance neutron production.[132] TW or

TABLE V. Comparison of neutron flux on the sample for certain applications at different neutron sources. Note that while the values for ILL are determined experimentally,[130] the values for ESS[127,128] and HBS[129] are from simulations, and for HBS as a first-of-its kind HiCANS, the instruments are not yet fully optimized.

ILL[130]	n/cm^2/s	ESS (2 MW)[127,128]	n/cm^2/s	HBS[129]	n/cm^2/s
D22	1.20×10^8	LOKI	4.00×10^8	SANS	4.10×10^7
Figaro	1.00×10^8	ESTIA	6.00×10^8	HorRef reflectometer	1.00×10^7
D20	9.80×10^7	DREAM	1.00×10^9	TPD diffractometer	1.60×10^8
IN5	6.80×10^5	CSPEC	4.00×10^6	CCS spectrometer	3.40×10^5
LADI	$1.10 \times 10^8 (1w)$	NMX	1.00×10^9	NMD diffractometer	1.80×10^7
NeXT	3.00×10^8	ODIN	1.20×10^9	C–NI imaging	3.00×10^6

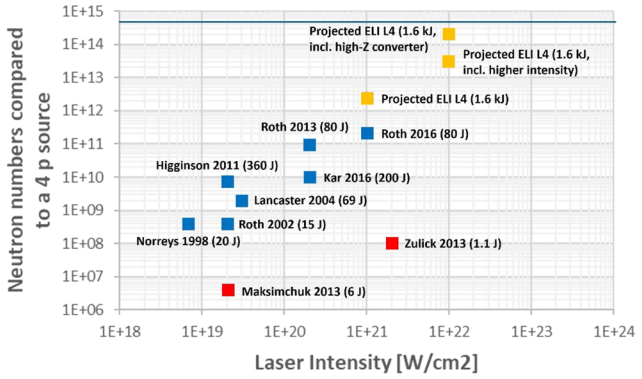

FIG. 6. Laser-driven neutron numbers vs laser intensity. The neutron numbers of the directed neutron beam per laser pulse are compared to a conventional isotropic (into 4π) neutron source. Results in red indicate short pulse lasers below 100 fs, blue are high energy lasers with around 0.5 ps pulse duration, and the yellow marks indicate the prospect for upcoming systems currently under construction. The top black line indicates the single, 250 ns pulse and neutron yield at the converter target, produced at the LANL LANSCE facility spallation source. [Reproduced and adapted with permission from Osvay *et al.*, Eur. Phys. J. Plus. **139**, 574 (2024). Copyright 2024 Author(s), licensed under a Creative Commons Attribution 4.0 license.]

PW systems trigger nuclear reactions with the resulting production of millions or billions of neutrons per laser pulse (Fig. 6). Large laser laboratories are able to produce 10^{10} n/pulse, whereas table-top systems generate a more modest fluence of some 10^{6} n/pulse.

With the use of solid target foils of submicrometer thickness and high contrast laser systems, the neutron yield has increased further by orders of magnitude compared to the earlier Target Normal Sheath Acceleration (TNSA) based attempts. With the enhancement of the laser contrast and the exploration of the relativistic transparency regime, laser-driven sources have now entered a per-pulse yield level that is on the level to reach out for real-world applications. The basic parameters of most current developed laser-driven neutron sources are summarized in Table VI.[133]

Based on the current experimental findings, a 200 J/10 Hz laser with high contrast could already provide around 10^{13} n/s. Due to the compact size of the system, the neutron flux density close to the converter could exceed 10^{20} n/cm^2/s.

B. Developments of targets/converters

The choice of an adequate target system strongly impacts the performance of an LDNS. The target has to be reasonably thin to benefit from the effects of relativistic induced transparency, stable, possible to produce in large quantities, and capable of operation at a high repetition rate. It also needs to be large enough to be reliably hit by the laser, and the target system has to survive the laser impact. For high repetition rates, it is also important that the target is mostly debris free. Furthermore, an operation with protons as well as with deuterons should be possible. In addition, the impact of target thickness can significantly affect the acceleration process. The number of limitations makes finding a suitable system not an easy task.[39]

1. Control of target material, heat deposition

The state of the art target technology for current LDNSs is deuterated polymer foils in the sub-μm regime. It was possible to reliably produce 5×10^{10} neutrons per single pulse at the PHELIX laser system.[134] These targets are produced by dissolving deuterated polystyrene in butanol and applying it via spin-coating to a flat silicon wafer. With a variation in rotation frequency and polymer concentration in the solution, the thickness can be tuned. For most experiments, these targets are exchanged manually and are replaced after each pulse. A solution is to attach the target foil to

TABLE VI. Parameters of laser-driven neutron sources at current. [Reproduced with permission from INTERNATIONAL ATOMIC ENERGY AGENCY, Compact Accelerator Based Neutron Sources, IAEA-TECDOC-1981, IAEA, Vienna, (2021).].

Neutron parameter	Parameter range
Spectrum	Energy range from thermal to >100 MeV Energy spread 100%
Neutrons per bunch	$>10^{10}$/sr (up to 2×10^{11} in 4π)
Spatial distribution	Isotropic component and fourfold enhanced forward beam
Opening angle	~90°
Forward neutrons	2×10^{10}/sr
Temporal structure	Bunch duration initially sub-nanosecond Repetition rate: equals the laser drive rate
Neutron generation scheme	Pitcher (deuterated plastic) + catcher (Be) + W reflector Deuteron-to-neutron conversion efficiency: $>10^{-2}$ Co-moving particles: e^- (MeV), gamma (MeV) Ions (depending on thickness of the converter) Target: Thin, deuterated foil (200–800 nm)
Laser parameter	Parameter range
Energy	0.1–500 J
Pulse duration	Picosecond

a target matrix where each hole is functioning as a single target. A prerequisite of this method is the protection of neighboring targets from debris and shock waves during a pulse, which could disturb the integrity of the thin foils. Solid plastic targets produce more debris than liquid targets, and the debris is often in the form of molten polystyrene, which coats nearby optics and parts of the final focusing parabola. This reduces the performance over time.[39] Similarly, polymer aerogel-foams with a mean density of 2 mg/cm^3 and submillimeter thickness of 6.2×10^{10} neutrons per single pulse were obtained.[135]

Overcoming the limit of matrix targets, a VHS tape for a TNSA target can be utilized. These tapes consist of 15 μm thick Mylar with embedded iron oxide particles and are placed on two spools. In between the spools, the tape is unwrapped and fixated in position by four highly polished stainless-steel bolts and can be targeted by the laser.[39] The main advantage of this system is its simplicity. A single VHS tape could last between 8000 and 20 000 pulses.

In order to minimize the debris of solid target materials, a laminar jet of cryogenic hydrogen as a target material can be used. The benefit of these jets is that they can theoretically operate without interruption as long as they have a sufficient supply of hydrogen and liquid helium as coolant. Using a deuterium jet also provides a pure D^+ beam without the contamination of protons.[39] A cryogenic hydrogen jet works by cooling H_2 or D_2 down to temperatures between 17 and 24 K inside a cryostat by the use of liquid helium to regulate the temperature. Experiments with cylindrical jets from 5 to 10 μm as well as rectangular jets with up to 2×40 μm have been conducted. With these latest results, the usage of a cryogenic jet might be promising for low energy, high-intensity laser systems.[39] An argument against this target type for an LDNS is the high degree of complexity and the early development stage.

To overcome the main difficulties of cryo-jets, the operation of liquid jets or synchronized droplets with water or ethylene glycol at room temperatures has been demonstrated. In the colliding leaf target system, two ethylene glycol jets collide at an angle, forming a liquid leaf. This target system enables a significantly higher hit rate as well as an increased pulse to pulse reproducibility. Under certain laser conditions, an upper repetition rate of 10 kHz could be reasonable. Hence, ethylene glycol liquid leaf jets represent a debris-free, sub µm, self-renewing target system for operation up to 1 kHz, respectively, 10 kHz, depending on the laser parameters.[39]

2. Catcher material

Lithium has the highest neutron gain for low proton energies below 15 MeV, while vanadium is optimal for high energetic ions. To gain an advantage from both materials, it is possible to create a stacked catcher with lithium in the front and vanadium or beryllium in the back. Stacked catchers produce more neutrons, which are also shifted to lower energies.[39]

Besides the catcher material, its geometry can also play an important role in maximizing the neutron yield. To move the neutron production further into the catcher, a recess in the shape of a cone can be drilled into the surface. Such a structure is known to reduce the backward flux for fast neutrons.[39]

C. Requirements on neutron moderation

While a few applications use high-energy neutrons, such as MeV neutron radiography, for most applications, epithermal or thermal energies are preferable. To provide neutrons with these energies, they have to be slowed down in a dedicated material.

As mentioned above, moderation of fast neutrons is based on energy loss during scattering reactions. Laser-driven neutron sources provide neutrons in the low-energy range due to the exponentially decaying spectrum. The goal of moderating laser-generated neutrons is to maximize the neutron yield in the desired energy range for the specific application. This includes the appropriate choice of the moderator material as well as its geometry and the right combination with an adequate catcher material and geometry, respectively.[134] In addition, moderators are placed within reflector materials (e.g., beryllium) to increase the neutron yield in the desired energy range by scattering fast neutrons back into the moderator.

Using nuclear reactions at lower energies, laser-driven ion sources can also produce softer neutron energy spectra because the ions at hundreds of keV to several MeV are produced in abundance with well-established ion acceleration methods. For instance, using near-threshold reaction via ^{7}Li(p,n)^{7}Be in TNSA, a fast neutron beam at around tens of keV has been achieved using a smaller moderator system with a shorter pulse duration.[105]

Moderators are designed to slow down neutrons without absorbing them. They contain light elements, such as hydrogen, deuterium, carbon, and beryllium, to maximize the mean energy loss per collision. On the other hand, the materials should exhibit low neutron capture cross sections to preserve a high neutron flux.

To moderate neutrons in the forward direction of a laser-driven neutron source, in a basic design, a graphite moderator has been placed directly behind the catcher.[134] As moderated neutrons are scattered in these directions, the low-energy neutron flux is enhanced. In another setup, high density polystyrene designed to slow down ~MeV neutrons to the epithermal range has been applied.[136]

By directing fast neutrons of above some MeV into a cryogenically cooled H2 moderator, a cold neutron flux of $\sim 2 \times 10^3$ n/cm^2/pulse was reached[105] (Fig. 7). The experiment demonstrated the feasibility of driving pulses of cold neutrons with short pulse lasers.

By placing the catcher within the moderator reflector assembly and using a compact arrangement similar to CANS and HiCANS, a very compact and efficient moderated neutron provision is feasible. Such a setup, arranging the catcher within the moderator, has been demonstrated,[112] minimizing the pulse duration of moderated neutrons in order to realize a time-of-flight spectroscopy over a short distance.

With the possibility of deploying samples in the proximity of the moderator and with the minimal radiation shielding requirement and the rising prospects of high repetition rate laser systems, laser-based sources could move further to reach a crucial stage in their development for being applied in neutron science and applications, and adequate sources might be placed at small laboratories in universities and industries.

D. Diagnostics/detectors

In the context of laser-driven neutrons, bubble detectors are widely used[68] for characterizing the neutron production, since they are insensitive to γ-rays and cover a large energy range from thermal to fast neutrons with a relatively flat response, and their electronics is not affected by EMP produced in the laser–plasma interaction.

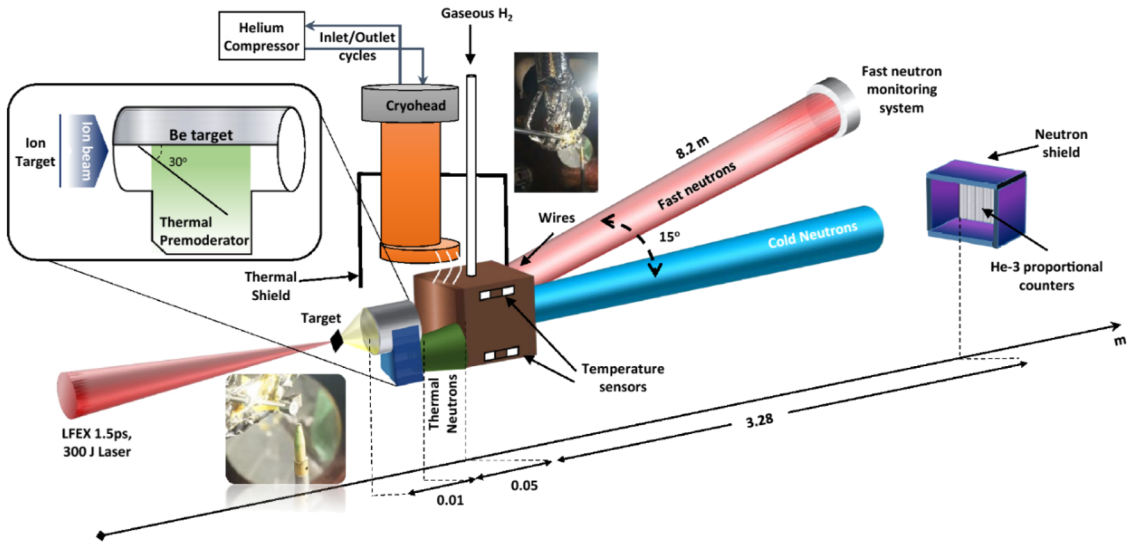

FIG. 7. Setup of the cold neutron source at the Osaka laser-driven neutron source (LDNS). [Reproduced with permission from Mirfayzi *et al.*, Sci. Rep. **10**, 20157 (2020). Copyright 2020 Author(s), licensed under a Creative Commons Attribution 4.0 license.]

Chemical Vapor Deposition (CVD) diamond detectors are applied most recently as they provide a faster response, making them a suitable choice for time-of-flight applications that require a high temporal resolution. In the case of fast neutrons, the electron–hole pairs are produced in the active body of the detector by the C recoils from neutron elastic scattering or by the products of nuclear reactions, such as $^{12}C(n,\alpha)$.[137]

In the case of detecting thermal or epithermal neutrons, a converter material is needed. Most often, materials containing boron or lithium are used to utilize the $^{10}B(n,\alpha)^{7}Li$ and the $^{6}Li(n,t)^{4}He$ reaction. Lithium glass scintillators are used, while boron is used inside borated micro-channel plates.

In addition, ^{3}He tubes utilize the $^{3}He(n,p)\,^{3}H$ reaction and are used widely for neutron scattering experiments but have lost relevance due to the high cost of ^{3}He. Thermal and epithermal neutron measurements often rely on time of flight measurements and, therefore, on event time tracking. New detector developments based on event mode data acquisition enable spatial and temporal tracking of neutron events at high efficiencies and moderate cost, significantly enhancing neutron-based measurement capabilities.[138] These detector types can achieve high resolutions below 100 μm and are mostly limited by the scintillator thickness, read-out pixel size, and source resolution.

For MeV neutron radiography, the most promising detector type is a combination of a scintillating screen coupled with an intensified gated camera system. As scintillators, typically organic scintillators based on polyvinyl toluene and stilbene crystals are used. The camera system needs to be outside the neutron beam to avoid radiation damage. For this reason, these detector types typically have a high-reflective mirror that enables placement of the camera at 90° toward the neutron beam. Prominent examples of this detector type have been developed by Mor *et al.*[139] Highly sensitive variants of this type utilize scintillating fibers to capture a higher fraction of neutrons during operation, typically at a cost of a spatial resolution, delivering a pixel size of 0.5–1 mm. Detector versions that aim for higher resolution utilize thin scintillating screens in the 100 μm range.

E. General technical risks

The materials mentioned for LDNS applicable for neutron generation also exhibit limiting factors on their overall applicability. Beryllium is toxic and can cause cancer if inhaled in the form of dust. As laser ion irradiation causes ablation at the catcher surface from the high velocity impact of the expanding plasma, this can cause pulverization of the beryllium surface and cause health hazards. For this reason, a beryllium catcher is usually protected by a thin, robust, and exchangeable ablation shield. As these shields stop a large fraction of the ions below 20 MeV, this reduces the total efficiency of a beryllium converter.[39] Additionally, beryllium is known to suffer from blistering, the formation of small hydrogen bubbles inside the material that leads to tensions and material failure over time. This problem is usually circumvented by reducing the beryllium thickness slightly below the stopping range so that the protons are stopped inside a material behind the converter, where the resulting hydrogen can be transported away. This is not possible with LDNS as the spectrum has a wide range of energies, all with different stopping ranges.

Lithium has to be shielded from air and moisture due to its high reactivity, or it is subject to rapid oxidation and material degradation. Even though in a vacuum chamber this does not cause severe problems, it excludes, for example, the simultaneous operation of a water-based liquid jet in combination with a lithium catcher.

The energy of the laser that is converted into fast ions will be deposited inside the catcher with every pulse. The heat transfer inside such a system is rather complex. With no air present in the vacuum chamber, the main contribution of a non-cooled system is

via radiative cooling of the front surface. The maximum surface temperature the catcher can have is equal to its melting temperature. For a lithium catcher with a 1.5 cm radius and the target chamber at 20 °C, this energy is only 1 mW due to the low emissivity and melting temperature.[39] Therefore, such laser systems with a repetition rate above 0.1 Hz are capable of reaching the melting point of lithium and require active cooling. Beryllium has a higher melting point at 1287 °C. Under similar conditions, the maximum repetition rate at which it could be operated without melting would be 5.1 kHz. For vanadium with an even higher melting temperature of 1910 °C, this repetition rate is further increased to 150 kHz. A thin stacked lithium–vanadium catcher with active cooling has shown the most promising results as a catcher for a high repetition neutron source.[39]

V. POTENTIAL FOR FUTURE LASER-DRIVEN NEUTRON SOURCES

For decades, neutron sources have shown their relevance and impact on the development of our science and innovation driven society. As a unique analytical tool to probe the structure and dynamics of matter in most developed countries, a sustainable and efficient ecosystem of neutron sources was established and used intensely. To tackle future challenges and requirements in our society, the continuous development and sustainable access to this ecosystem of neutron sources have to be maintained.[4,140]

The possibility of developing a thermal neutron source with ultra-short neutron pulses could be of interest for ultrafast dynamic studies in material science and condensed matter physics. In fusion energy research, ultrafast studies may allow us to trigger and visualize in real time the production and evolution of radiation damage at the atomic scale. Short bursts of neutrons would also be a powerful probe to obtain crucial information about the state of matter under extreme conditions, such as those found in inertial confinement fusion.[101] In addition, an interesting application would be the use of a compact source of pulsed, mono-energetic MeV neutrons delivering above 10^{10} n/cm^2/s for security measures at checkpoints for investigation of large cargo containers by using the MeV neutron radiography technique, where the nature and location of the threat can be identified by simultaneously measuring scattered neutrons and time of flight of the induced gamma radiations.[101]

The different communities have to be merged to harvest synergies between, for example, the laser and neutron communities at universities and facilities. Based on recent progress and future developments, a benchmark demonstrator of a laser-driven neutron source/beamline to prove the maturity of the approach is highly desirable. A dedicated facility for future research and development could be realized with such a demonstrator, opening new perspectives and applications with neutrons.

Laser-driven neutron sources are an exciting new opportunity for neutron research.[5,6] Based on the technical and scientific descriptions given here, one can distinguish between applications requiring

(i) a high average flux of thermal neutrons in a large volume (e.g., radionuclide production, silicon doping, and radiation damage studies),
(ii) precision physics, mostly with high density of ultracold neutrons (e.g., studies of neutron lifetime, neutron electric dipole moment, gravitational physics, etc),
(iii) application of epithermal and high energy neutrons (e.g., for imaging and analytics),
(iv) various specialized uses of neutron beams [for example, materials testing for fusion reactor cladding or medical applications, such as Boron Neutron Capture Therapy (BNCT), which is not yet available in Europe but is enjoying a fast growth in Japan],
(v) high brightness cold, thermal, and epithermal neutron beams for beamline instruments (e.g., materials and active agent research with diffractometers, large scale structure instruments, imaging, analytics, and spectrometers), and
(vi) combination of x-ray/neutron imaging with the high spatial resolution of x rays and the hydrogen sensitivity of neutrons.

Looking at the current situation,

(i) Applications requiring high average neutron flux are by far best realized in the water moderator of a research reactor. Accelerator- or laser-driven sources are most efficient in pulsed operation, where high peak fluxes can be achieved, while the source strength, as a time-averaged parameter, generally lags behind that of high-flux research reactors, with the exception of large flagship facilities, such as the ESS. However, facilities using high-energy proton beams offer some additional possibilities compared to research reactors, namely, the production of radionuclides produced by proton-induced reactions.
(ii) Applications in precision physics can be realized in both research reactors and accelerator-driven sources, since cold neutrons can be stored, and high densities can be achieved by successive filling from a pulsed source.
(iii) Applications of epithermal and high energy neutrons for imaging and analytics are still underrepresented, mainly because the research reactors with their water tanks, which have been the most common sources in Europe, were not well-suited to provide intense beams of high energy neutrons.

This situation might change significantly in the coming years. Both HiCANS and laser-driven sources are well-suited to provide the necessary beams. High energy neutrons are very penetrating. They offer enormous potential for quality control in the manufacture of large, expensive engineering structures and for elemental analysis in the raw materials and recycling industries. The combination of imaging and time-of-flight elemental analysis requires very short pulses in the μs to ns range. Such pulses can be realized for high-energy neutrons where no moderator is present. This is the domain of laser-driven sources, whereas linacs do not yet reach the sub-nanosecond pulse regime.
(iv) Applications of high-brightness thermal neutron beams, it is fair to say that laser-driven neutron sources are not yet competitive with sources driven by conventional accelerators. Compared to HiCANS, they will provide several orders of magnitude lower flux at the sample. At present, two features, in particular, hinder the efficient production of useful neutron beams for these applications: the rather broad energy spectrum of the protons hitting the converter, which makes the optimization of the converter difficult, and the short pulses, which are not long enough to efficiently feed the

moderators. These aspects can be addressed in development projects.

The rapid increase in the performance of modern laser systems offers the prospect that such systems can drive small local neutron sources for training of students, method development, and dedicated experiments, e.g., SANS or neutron imaging. Opportunities exist for groups at universities or research institutions with expertise in both laser systems and neutron beam applications to advance the development of laser-driven CANS.

VI. CONCLUSION

In summary, laser-driven neutron sources already provide exciting opportunities for imaging, scattering, and analytics with epithermal and high energy neutron beams. In-depth development efforts are needed to demonstrate the usefulness of such sources for materials science applications that rely on cold, thermal, and epithermal neutron beams. These efforts are best undertaken at small laser-driven compact neutron sources (LD-CaNSs), while for the foreseeable future, larger neutron user facilities will be best served by conventional accelerator technologies.

AUTHOR DECLARATIONS

Conflict of Interest

The authors have no conflicts to disclose.

Author Contributions

T. Gutberlet: Conceptualization (lead); Visualization (lead); Writing – original draft (lead); Writing – review & editing (lead). **M. Bleuel**: Data curation (equal); Writing – original draft (equal); Writing – review & editing (equal). **T. Brückel**: Resources (equal); Writing – original draft (equal); Writing – review & editing (equal). **L. G. Butler**: Data curation (equal); Investigation (equal); Writing – original draft (equal); Writing – review & editing (equal). **C. Guerrero**: Investigation (equal); Writing – original draft (equal); Writing – review & editing (equal). **T. T. Jäger**: Writing – original draft (equal); Writing – review & editing (equal). **G. Muhrer**: Conceptualization (equal); Validation (equal); Writing – original draft (equal); Writing – review & editing (equal). **S. Scheuren**: Investigation (equal); Writing – original draft (equal); Writing – review & editing (equal). **A. Schreyer**: Conceptualization (equal); Resources (equal); Writing – original draft (equal); Writing – review & editing (equal). **S. C. Vogel**: Conceptualization (equal); Investigation (equal); Validation (equal); Writing – original draft (equal); Writing – review & editing (equal). **K. Zeil**: Investigation (equal); Writing – original draft (equal); Writing – review & editing (equal).

DATA AVAILABILITY

The data used to support the findings of this study are available from the authors upon reasonable request.

NOMENCLATURE

BNCT	boron neutron capture therapy
CANS	compact accelerator-based neutron source
CVD	chemical vapor deposition
CW	constant wave
DNAA	delayed neutron activation analysis
HiCANS	high-current accelerator-based neutron source
ICF	inertial confinement fusion
LDNS	laser-driven neutron sources
LWFA	laser wakefield acceleration
NAA	neutron activation analysis
NRS	neutron resonance spectroscopy
NRTA	neutron resonance transmission analysis
PGNAA	prompt gamma neutron activation analysis
RFQ	radio-frequency quadrupole
SANS	small angle neutron scattering
SEE	single event effect
TNSA	target-normal sheaths acceleration

REFERENCES

[1] V. V. Kuznov and S. V. Ryzhkov, "Small-sized plasma generators—Sources of high-energy particle and neutron fluxes," Fusion Sci. Technol. **81**, 789 (2025).

[2] M. Arai and K. Crawford, "Neutron sources and facilities," in *Neutron Imaging and Applications*, *Neutron Scattering Applications and Techniques*, edited by H. Bilheux, R. McGreevy, and I. Anderson (Springer, Boston, 2009).

[3] G. S. Bauer, "Physics and technology of spallation neutron sources," Nucl. Instrum. Methods Phys. Res., Sect. A **463**, 505–543 (2001).

[4] P. Zakalek, T. Gutberlet, and T. Brückel, "Neutron sources for large scale user facilities: The potential of high current accelerator-driven neutron sources," Prog. Part. Nucl. Phys. **142**, 104163 (2025).

[5] A. Yogo, Y. Arikawa, Y. Abe, S. R. Mirfayzi, T. Hayakawa, K. Mima, and R. Kodama, "Advances in laser-driven neutron sources and applications," Eur. Phys. J. A **59**, 191 (2023).

[6] M. Zimmer, T. F. Rösch, S. Scheuren, T. Seupel, T. Jäger, J. Kohl, D. Hofmann, G. Schaumann, and M. Roth, "Assessing the potential of upcoming laser-driven neutron sources and their practical applications for industry and society," Eur. Phys. J. Plus **139**, 1107 (2024).

[7] X. R. Jiang, F. Q. Shao, D. B. Zou, M. Y. Yu, L. X. Hu, X. Y. Guo, T. W. Huang, H. Zhang, S. Z. Wu, G. B. Zhang, T. P. Yu, Y. Yin, H. B. Zhuo, and C. T. Zhou, "Energetic deuterium-ion beams and neutron source driven by multiple-laser interaction with pitcher-catcher target," Nucl. Fusion **60**, 076019 (2020).

[8] T. Ditmire, J. Zweiback, V. P. Yanovsky, T. E. Cowan, G. Hays, and K. B. Wharton, "Nuclear fusion from explosions of femtosecond laser-heated deuterium clusters," Nature **398**(6727), 489–492 (1999).

[9] International Atomic Energy Agency, "Handbook on photonuclear data for applications cross-sections and spectra," Report No. IAEA-TECDOC-1178, IAEA, Vienna, 2000, https://www.iaea.org/publications/6043/handbook-on-photonuclear-data-for-applications-cross-sections-and-spectra.

[10] R. E. Lapp and H. L. Andrews, *Nuclear Radiation Physics* (Prentice-Hall, Englewood Cliffs, NJ, 1972).

[11] W. P. Swanson, "Improved calculation of photoneutron yields released by incident electrons," Health Phys. **37**(3), 347–358 (1979).

[12] J. S. Levinger, "Theories of photonuclear reactions," Annu. Rev. Nucl. Sci. **4**(1), 13–32 (1954).

[13] G. C. Baldwin and G. S. Klaiber, "Photo-fission in heavy elements," Phys. Rev. **71**(1), 3 (1947).

[14] R. O. Haxby, W. E. Shoupp, W. E. Stephens, and W. H. Wells, "Photo-fission of uranium and thorium," Phys. Rev. **59**(1), 57 (1941).

[15] S. P. Hatchett, C. G. Brown, T. E. Cowan, E. A. Henry, J. S. Johnson, M. H. Key, J. A. Koch, A. B. Langdon, B. F. Lasinski, R. W. Lee, A. J. Mackinnon, D. M. Pennington, M. D. Perry, T. W. Phillips, M. Roth, T. C. Sangster, M. S. Singh, R. A. Snavely, M. A. Stoyer, S. C. Wilks, and K. Yasuike, "Electron, photon, and ion beams from the relativistic interaction of petawatt laser pulses with solid targets," Phys. Plasmas **7**(5), 2076–2082 (2000).

[16] S. C. Wilks, A. B. Langdon, T. E. Cowan, M. Roth, M. Singh, S. Hatchett, M. H. Key, D. Pennington, A. MacKinnon, and R. A. Snavely, "Energetic proton

generation in ultra-intense laser–solid interactions," Phys. Plasmas **8**(2), 542–549 (2001).
[17]A. Higginson, R. J. Gray, M. King, R. J. Dance, S. D. R. Williamson, N. M. H. Butler, R. Wilson, R. Capdessus, C. Armstrong, J. S. Green, S. J. Hawkes, P. Martin, W. Q. Wei, S. R. Mirfayzi, X. H. Yuan, S. Kar, M. Borghesi, R. J. Clarke, D. Neely, and P. McKenna, "Near-100 MeV protons via a laser-driven transparency-enhanced hybrid acceleration scheme," Nat. Commun. **9**, 724 (2018).
[18]T. Ziegler, I. Göthel, S. Assenbaum, C. Bernert, F.-E. Brack, T. E. Cowan, N. P. Dover, L. Gaus, T. Kluge, S. Kraft, F. Kroll, J. Metzkes-Ng, M. Nishiuchi, I. Prencipe, T. Püschel, M. Rehwald, M. Reimold, H.-P. Schlenvoigt, M. E. P. Umlandt, M. Vescovi, U. Schramm, and K. Zeil, "Laser-driven high-energy proton beams from cascaded acceleration regimes," Nat. Phys. **20**, 1211 (2024).
[19]J. R. Oppenheimer, "The disintegration of the deuteron by impact," Phys. Rev. **47**(11), 845 (1935).
[20]R. Serber, "The production of high energy neutrons by stripping," Phys. Rev. **72**(11), 1008 (1947).
[21]M. Roth, D. Jung, K. Falk, N. Guler, O. Deppert, M. Devlin, A. Favalli, J. Fernandez, D. Gautier, M. Geissel, R. Haight, C. E. Hamilton, B. M. Hegelich, R. P. Johnson, F. Merrill, G. Schaumann, K. Schoenberg, M. Schollmeier, T. Shimada, T. Taddeucci, J. L. Tybo, F. Wagner, S. A. Wender, C. H. Wilde, and G. A. Wurden, "Bright laser-driven neutron source based on the relativistic transparency of solids," Phys. Rev. Lett. **110**(4), 044802 (2013).
[22]J. C. Fernández, D. Cort Gautier, C. Huang, S. Palaniyappan, B. J. Albright, W. Bang, G. Dyer, A. Favalli, J. F. Hunter, J. Mendez, M. Roth, M. Swinhoe, P. A. Bradley, O. Deppert, M. Espy, K. Falk, N. Guler, C. Hamilton, B. M. Hegelich, D. Henzlova, K. D. Ianakiev, M. Iliev, R. P. Johnson, A. Kleinschmidt, A. S. Losko, E. McCary, M. Mocko, R. O. Nelson, R. Roycroft, M. A. Santiago Cordoba, V. A. Schanz, G. Schaumann, D. W. Schmidt, A. Sefkow, T. Shimada, T. N. Taddeucci, A. Tebartz, S. C. Vogel, E. Vold, G. A. Wurden, and L. Yin, "Laser-plasmas in the relativistic-transparency regime: Science and applications," Phys. Plasmas **24**(5), 056702 (2017).
[23]L. Yin, B. Albright, B. Hegelich, and J. C. Fernández, "GeV laser ion acceleration from ultrathin targets: The laser break-out afterburner," Laser Part. Beams **24**(2), 291–298 (2006).
[24]B. M. Hegelich, I. Pomerantz, L. Yin, H. C. Wu, D. Jung, B. J. Albright, D. C. Gautier, S. Letzring, S. Palaniyappan, R. Shah, K. Allinger, R. Hörlein, J. Schreiber, D. Habs, J. Blakeney, G. Dyer, L. Fuller, E. Gaul, E. Mccary, A. R. Meadows, C. Wang, T. Ditmire, and J. C. Fernandez, "Laser-driven ion acceleration from relativistically transparent nanotargets," New J. Phys. **15**(8), 085015 (2013).
[25]M. Gauthier, C. B. Curry, S. Göde, F.-E. Brack, J. B. Kim, M. J. MacDonald, J. Metzkes, L. Obst, M. Rehwald, C. Rödel, H.-P. Schlenvoigt, W. Schumaker, U. Schramm, K. Zeil, and S. H. Glenzer, "High repetition rate, multi-MeV proton source from cryogenic hydrogen jets," Appl. Phys. Lett. **111**(11), 114102 (2017).
[26]M. Rehwald, S. Assenbaum, C. Bernert, F.-E. Brack, M. Bussmann, T. E. Cowan, C. B. Curry, F. Fiuza, M. Garten, L. Gaus, M. Gauthier, S. Göde, I. Göthel, S. H. Glenzer, L. Huang, A. Huebl, J. B. Kim, T. Kluge, S. Kraft, F. Kroll, J. Metzkes-Ng, T. Miethlinger, M. Loeser, L. Obst-Huebl, M. Reimold, H.-P. Schlenvoigt, C. Schoenwaelder, U. Schramm, M. Siebold, F. Treffert, L. Yang, T. Ziegler, and K. Zeil, "Ultra-short pulse laser acceleration of protons to 80 MeV from cryogenic hydrogen jets tailored to near-critical density," Nat. Commun. **14**, 4009 (2023).
[27]F. Treffert, C. Curry, T. Ditmire, G. Glenn, H. Quevedo, M. Roth, C. Schoenwaelder, M. Zimmer, S. Glenzer, and M. Gauthier, "Towards high-repetition-rate fast neutron sources using novel enabling technologies," Instruments **5**(4), 38 (2021).
[28]T. Tajima and J. M. Dawson, "Laser electron accelerator," Phys. Rev. Lett. **43**(4), 267 (1979).
[29]J. Wenz and S. Karsch, "Physics of laser-wakefield accelerators (LWFA)," arXiv:2007.04622 (2020).
[30]J. Osterhoff, A. Popp, Z. Major, B. Marx, T. P. Rowlands-Rees, M. Fuchs, M. Geissler, R. Hörlein, B. Hidding, S. Becker, E. A. Peralta, U. Schramm, F. Grüner, D. Habs, F. Krausz, S. M. Hooker, and S. Karsch, "Generation of stable, low-divergence electron beams by laser-wakefield acceleration in a steady-state-flow gas cell," Phys. Rev. Lett. **101**(8), 085002 (2008).
[31]S. Banerjee, N. D. Powers, V. Ramanathan, I. Ghebregziabher, K. J. Brown, C. M. Maharjan, S. Chen, A. Beck, E. Lefebvre, S. Y. Kalmykov, B. A. Shadwick, and D. P. Umstadter, "Generation of tunable, 100–800 MeV quasi-monoenergetic electron beams from a laser-wakefield accelerator in the blowout regime," Phys. Plasmas **19**(5), 056703 (2012).
[32]M. Filippova, B. Holzer, Y. Papaphilippou, D. Rivoiron, H. Schmickler, and F. Tecker, in *Proceedings of the 2019 course on High Gradient Wakefield Accelerators, Sesimbra, Portugal, 11–22 March 2019* (CERN, 2020).
[33]A. Gonsalves, K. Nakamura, J. Daniels, C. Benedetti, C. Pieronek, T. De Raadt, S. Steinke, J. Bin, S. Bulanov, J. Van Tilborg, C. G. R. Geddes, C. B. Schroeder, C. Tóth, E. Esarey, K. Swanson, L. Fan-Chiang, G. Bagdasarov, N. Bobrova, V. Gasilov, G. Korn, P. Sasorov, and W. P. Leemans, "Petawatt laser guiding and electron beam acceleration to 8 GeV in a laser-heated capillary discharge waveguide," Phys. Rev. Lett. **122**(8), 084801 (2019).
[34]S. Scheuren, T. Jäger, J. Kohl, S. Kuschel, T. F. Rösch, B. Schmitz, M. Zimmer, C. Rödel, and M. Roth, "Scaling of laboratory neutron sources based on laser wakefield-accelerated electrons using Monte Carlo simulations," Eur. Phys. J. Plus **139**, 726 (2024).
[35]D. Papp, A. Necas, N. Hafz, T. Tajima, S. Gales, G. Mourou, G. Szabo, and C. Kamperidis, "Laser wakefield photoneutron generation with few-cycle high-repetition-rate laser systems," Photonics **9**(11), 826 (2022).
[36]D. Papp, Z. Lécz, C. Kamperidis, and N. A. M. Hafz, "Highly efficient few-cycle laser wakefield electron accelerator," Plasma Phys. Controlled Fusion **63**(6), 065019 (2021).
[37]J. Feng, C. Fu, Y. Li, X. Zhang, J. Wang, D. Li, C. Zhu, J. Tan, M. Mirzaie, Z. Zhang, and L. Chen, "High-efficiency neutron source generation from photonuclear reactions driven by laser plasma accelerator," High Energy Density Phys. **36**, 100753 (2020).
[38]W. P. Leemans, D. Rodgers, P. E. Catravas, C. G. R. Geddes, G. Fubiani, E. Esarey, B. A. Shadwick, R. Donahue, and A. Smith, "Gamma-neutron activation experiments using laser wakefield accelerators," Phys. Plasmas **8**(5), 2510–2516 (2001).
[39]M. Zimmer, "Laser-driven neutron sources–A compact approach to non-destructive material analysis," Ph.D. dissertation (Technische Universität Darmstadt, 2020).
[40]C. B. Curry, C. Schoenwaelder, S. Goede, J. B. Kim, M. Rehwald, F. Treffert, K. Zeil, S. H. Glenzer, and M. Gauthier, "Cryogenic liquid jets for high repetition rate discovery science," J. Visualized Exp. **159**, e61130 (2020).
[41]M. Rehwald, S. Assenbaum, C. Bernert, C. B. Curry, M. Gauthier, S. H. Glenzer, S. Göde, C. Schoenwaelder, U. Schramm, F. Treffert, and K. Zeil, "Towards high-repetition rate petawatt laser experiments with cryogenic jets using a mechanical chopper system," J. Phys.: Conf. Ser. **2420**(1), 012034 (2023).
[42]K. Nakajima, T. Kawakubo, H. Nakanishi, A. Ogata, Y. Kato, Y. Kitagawa, R. Kodama, K. Mima, H. Shiraga, K. Suzuki, T. Zhang, Y. Sakawa, T. Shoji, Y. Nishida, N. Yugami, M. Downer, D. Fisher, B. Newberger, and T. Tajima, "A proof-of-principle experiment of laser wakefield acceleration," Phys. Scr. **1994**(T52), 61.
[43]A. Ting, C. I. Moore, K. Krushelnick, C. Manka, E. Esarey, P. Sprangle, R. Hubbard, H. R. Burris, R. Fischer, and M. Baine, "Plasma wakefield generation and electron acceleration in a self-modulated laser wakefield accelerator experiment," Phys. Plasmas **4**(5), 1889–1899 (1997).
[44]S. Kuschel, M. Schwab, M. Yeung, D. Hollatz, A. Seidel, W. Ziegler, A. Sävert, M. Kaluza, and M. Zepf, "Controlling the self-injection threshold in laser wakefield accelerators," Phys. Rev. Lett. **121**(15), 154801 (2018).
[45]S. Jalas, M. Kirchen, C. Braun, T. Eichner, J. Gonzalez, L. Hübner, T. Hülsenbusch, P. Messner, G. Palmer, M. Schnepp, C. Werle, P. Winkler, W. P. Leemans, and A. R. Maier, "Tuning curves for a laser-plasma accelerator," Phys. Rev. Accel. Beams **26**(7), 071302 (2023).
[46]A. R. Maier, N. M. Delbos, T. Eichner, L. Hübner, S. Jalas, L. Jeppe, S. W. Jolly, M. Kirchen, V. Leroux, P. Messner, M. Schnepp, M. Trunk, P. A. Walker, C. Werle, and P. Winkler, "Decoding sources of energy variability in a laser-plasma accelerator," Phys. Rev. X **10**(3), 031039 (2020).
[47]D. Gustas, D. Guénot, A. Vernier, S. Dutt, F. Böhle, R. Lopez-Martens, A. Lifschitz, and J. Faure, "High-charge relativistic electron bunches from a kHz laser-plasma accelerator," Phys. Rev. Accel. Beams **21**(1), 013401 (2018).
[48]Z.-H. He, A. G. R. Thomas, B. Beaurepaire, J. A. Nees, B. Hou, V. Malka, K. Krushelnick, and J. Faure, "Electron diffraction using ultrafast electron bunches

from a laser-wakefield accelerator at kHz repetition rate," Appl. Phys. Lett. **102**(6), 064104 (2013).
[49]H. Kiriyama, Y. Miyasaka, A. Kon, M. Nishiuchi, A. Sagisaka, H. Sasao, A. S. Pirozhkov, Y. Fukuda, K. Ogura, K. Kondo, N. Nakanii, Y. Mashiba, N. P. Dover, L. Chang, M. Kando, S. Bock, T. Ziegler, T. Püschel, H.-P. Schlenvoigt, K. Zeil, and U. Schramm, "Laser output performance and temporal quality enhancement at the J-KAREN-P petawatt laser facility," Photonics **10**(9), 997 (2023).
[50]G. A. Mourou, G. Korn, J. L. Sandner, and W. Collier, "Science and technology with ultra-intense lasers," in *ELI-Extreme Light Infrastructure: Whitebook* (THOSS Media GmbH, 2011).
[51]E. Sistrunk, D. A. Alessi, A. Bayramian, K. Chesnut, A. Erlandson, T. C. Galvin, D. Gibson, H. Nguyen, B. Reagan, K. Schaffers, C. W. Siders, T. Spinka, and C. Haefner, "Laser technology development for high peak power lasers achieving kilowatt average power and beyond," Proc. SPIE **11034**, 1103407 (2019).
[52]J. T. Morrison, S. Feister, K. D. Frische, D. R. Austin, G. K. Ngirmang, N. R. Murphy, C. Orban, E. A. Chowdhury, and W. M. Roquemore, "MeV proton acceleration at kHz repetition rate from ultra-intense laser liquid interaction," New J. Phys. **20**(2), 022001 (2018).
[53]S. Ikeda, M. Okamura, T. Kanesue, D. Raparia, A. Hershcovitch, K. Yip, K. Takahashi, D. Wu, A. Cannavò, and G. Ceccio, "Neutron generator based on intense lithium beam driver," Rev. Sci. Instrum. **91**(2), 023304 (2020).
[54]A. S. Tremsin, J. B. McPhate, J. V. Vallerga, O. H. W. Siegmund, W. B. Feller, H. Z. Bilheux, J. J. Molaison, C. A. Tulk, L. Crow, R. G. Cooper, and D. Penumadu, "Transmission Bragg edge spectroscopy measurements at ORNL spallation neutron source," J. Phys.: Conf. Ser. **251**, 012069 (2010).
[55]R. Garoby, A. Vergara, H. Danared, I. Alonso, E. Bargallo, B. Cheymol, C. Darve, M. Eshraqi, H. Hassanzadegan, A. Jansson, I. Kittelmann, Y. Levinsen, M. Lindroos, C. Martins, Ø. Midttun, R. Miyamoto, S. Molloy, D. Phan, A. Ponton, E. Sargsyan, T. Shea, A. Sunesson, L. Tchelidze, C. Thomas, M. Jensen, W. Hees, P. Arnold, M. Juni-Ferreira, F. Jensen, A. Lundmark, D. McGinnis, N. Gazis, J. Weisend II, M. Anthony, E. Pitcher, L. Coney, M. Gohran, J. Haines, R. Linander, D. Lyngh, U. Oden, H. Carling, R. Andersson, S. Birch, J. Cereijo, T. Friedrich, T. Korhonen, E. Laface, M. Mansouri-Sharifabad, A. Monera-Martinez, A. Nordt, D. Paulic, D. Piso, S. Regnell, M. Zaera-Sanz, M. Aberg, K. Breimer, K. Batkov, Y. Lee, L. Zanini, M. Kickulies, Y. Bessler, J. Ringnér, J. Jurns, A. Sadeghzadeh, P. Nilsson, M. Olsson, J.-E. Presteng, H. Carlsson, A. Polato, J. Harborn, K. Sjögreen, G. Muhrer, and F. Sordo, "The European spallation source design," Phys. Scr. **93**, 014001 (2017).
[56]S. H. Batha, R. Aragonez, F. L. Archuleta, T. N. Archuleta, J. F. Benage, J. A. Cobble, J. S. Cowan, V. E. Fatherley, K. A. Flippo, D. C. Gautier, R. P. Gonzales, S. R. Greenfield, B. M. Hegelich, T. R. Hurry, R. P. Johnson, J. L. Kline, S. A. Letzring, E. N. Loomis, F. E. Lopez, S. N. Luo, D. S. Montgomery, J. A. Oertel, D. L. Paisley, S. M. Reid, P. G. Sanchez, A. Seifter, T. Shimada, and J. B. Workman, "TRIDENT high-energy-density facility experimental capabilities and diagnostics," Rev. Sci. Instrum. **79**(10), 10F305 (2008).
[57]M. Martinez, W. Bang, G. Dyer, X. Wang, E. Gaul, T. Borger, M. Ringuette, M. Spinks, H. Quevedo, A. Bernstein, M. Donovan, and T. Ditmire, "The Texas petawatt laser and current experiments," AIP Conf. Proc. **1507**, 874–878 (2012).
[58]V. Bagnoud, B. Aurand, A. Blazevic, S. Borneis, C. Bruske, B. Ecker, U. Eisenbarth, J. Fils, A. Frank, E. Gaul, S. Goette, C. Haefner, T. Hahn, K. Harres, H.-M. Heuck, D. Hochhaus, D. H. H. Hoffmann, D. Javorková, H.-J. Kluge, T. Kuehl, S. Kunzer, M. Kreutz, T. Merz-Mantwill, P. Neumayer, E. Onkels, D. Reemts, O. Rosmej, M. Roth, T. Stoehlker, A. Tauschwitz, B. Zielbauer, D. Zimmer, and K. Witte, "Commissioning and early experiments of the PHELIX facility," Appl. Phys. B **100**, 137–150 (2010).
[59]C. Hernandez-Gomez, P. A. Brummitt, D. J. Canny, R. J. Clarke, J. Collier, C. N. Danson, A. M. Dunne, B. Fell, A. J. Frackiewicz, S. Hancock, S. Hawkes, R. Heathcote, P. Holligan, M. H. R. Hutchinson, A. Kidd, W. J. Lester, I. O. Musgrave, D. Neely, D. R. Neville, P. A. Norreys, D. A. Pepler, C. J. Reason, W. Shaikh, T. B. Winstone, and B. E. Wyborn, "Vulcan petawatt-operation and development," J. Phys. IV **133**, 555–559 (2006).
[60]U. Schramm, M. Bussmann, A. Irman, M. Siebold, K. Zeil, D. Albach, C. Bernert, S. Bock, F. Brack, J. Branco, J. Couperus, T. Cowan, A. Debus, C. Eisenmann, M. Garten, R. Gebhardt, S. Grams, U. Helbig, A. Huebl, T. Kluge, A. Köhler, J. Krämer, S. Kraft, F. Kroll, M. Kuntzsch, U. Lehnert, M. Loeser, J. Metzkes, P. Michel, L. Obst, R. Pausch, M. Rehwald, R. Sauerbrey, H. Schlenvoigt, K. Steiniger, and O. Zarini, "First results with the novel petawatt laser acceleration facility in Dresden," J. Phys.: Conf. Ser. **874**, 012028 (2017).
[61]W. P. Leemans, R. Duarte, E. Esarey, S. Fournier, C. G. R. Geddes, D. Lockhart, C. B. Schroeder, C. Toth, J. Vay, and S. Zimmermann, "The Berkeley lab laser accelerator (BELLA): A 10 GeV laser plasma accelerator," AIP Conf. Proc. **1299**, 3–11 (2010).
[62]Y. Wang, S. Wang, A. Rockwood, B. M. Luther, R. Hollinger, A. Curtis, C. Calvi, C. S. Menoni, and J. J. Rocca, "0.85 PW laser operation at 3.3 Hz and high-contrast ultrahigh-intensity λ = 400 nm second-harmonic beamline," Opt. Lett. **42**, 3828–3831 (2017).
[63]N. Guler, P. Volegov, A. Favalli, F. E. Merrill, K. Falk, D. Jung, J. L. Tybo, C. H. Wilde, S. Croft, C. Danly, O. Deppert, M. Devlin, J. Fernandez, D. C. Gautier, M. Geissel, R. Haight, C. E. Hamilton, B. M. Hegelich, D. Henzlova, R. P. Johnson, G. Schaumann, K. Schoenberg, M. Schollmeier, T. Shimada, M. T. Swinhoe, T. Taddeucci, S. A. Wender, G. A. Wurden, and M. Roth, "Neutron imaging with the short-pulse laser driven neutron source at the Trident laser facility," J. Appl. Phys. **120**, 154901 (2016).
[64]W. Bang, G. Dyer, H. J. Quevedo, A. C. Bernstein, E. Gaul, M. Donovan, and T. Ditmire, "Optimization of the neutron yield in fusion plasmas produced by Coulomb explosions of deuterium clusters irradiated by a petawatt laser," Phys. Rev. E **87**, 023106 (2013).
[65]A. Kleinschmidt, V. Bagnoud, O. Deppert, A. Favalli, S. Frydrych, J. Hornung, D. Jahn, G. Schaumann, A. Tebartz, F. Wagner, G. Wurden, B. Zielbauer, and M. Roth, "Intense, directed neutron beams from a laser-driven neutron source at PHELIX," Phys. Plasmas **25**, 053101 (2018).
[66]R. Singhal, P. Norreys, and H. Habara, "Nuclear physics with intense lasers," in *Strong Field Laser Physics*, edited by T. Brabec (Springer Science & Business Media, 2008), pp. 519–536.
[67]M. Tisi, "Secondary neutrons at laser-driven ion sources," Ph.D. dissertation (Ludwig-Maximilians-Universität München, 2022).
[68]R. Lelièvre, W. Yao, T. Waltenspiel, I. Cohen, V. Anthonippillai, P. Antici, A. Beck, E. Cohen, D. Michaeli, I. Pomerantz, D. C. Gautier, F. Trompier, Q. Ducasse, P. Koseoglou, P.-A. Soderstrom, F. Mathieu, A. Allaoua, and J. Fuchs, "A comprehensive characterization of the neutron fields produced by the Apollon petawatt laser," Eur. Phys. J. Plus **139**, 1035 (2024).
[69]T. Schenkel, Q. Ji, A. Persaud, P. A. Seidl, S. Steinke, K. Nakamura, and W. P. Leemans, "Intense, pulsed ion beams for radiation effects research at Berkeley Lab," Report No. LLNL-CONF-758685, Hardened Electronics and Radiation Technology, 2018.
[70]R. Lelièvre, E. Catrix, S. Vallières, S. Fourmaux, A. Allaoua, V. Anthonippillai, P. Antici, Q. Ducasse, and J. Fuchs, "High repetition-rate 0.5 Hz broadband neutron source driven by the Advanced Laser Light Source," Phys. Plasmas **31**, 093106 (2024).
[71]F. S. Treffert, J. G. Williams, T. Ma, C. B. Curry, D. Deponte, G. Jain, M. Gauthier, G. Glenn, S. H. Glenzer, C. Schoenwaelder, R. C. Hollinger, J. J. Rocca, B. Sullivan, S. Wang, S. Z. Anaraki, S. Popa, D. Ursescu, T. Ditmire, H. J. Quevedo, M. Roth, and M. Zimmer, "High flux directional laser driven neutron sources for static radiography applications," in 65th Annual Meeting of the APS Division of Plasma Physics, 2023, https://meetings.aps.org/Meeting/DPP23/Session/CO08.11.
[72]K. Osvay, L. Stuhl, P. Varmazyar, T. Gilinger, Z. Elekes, A. Fenyvesi, K. Hideghethy, R. E. Szabo, M. Füle, B. Biró, Z. Halász, Z. Halász, I. Kuti, R. Molnár, A. Ébert, A. Ébert, E. Buzás, E. Buzás, P. K. Singh, S. Hussain, A. Börzsönyi, Z. Fülöp, Z. Fülöp, G. Mourou, G. Szabó, and G. Szabó, "Towards a 10^{10} n/s neutron source with kHz repetition rate, few-cycle laser pulses," Eur. Phys. J. Plus **139**, 574 (2024).
[73]L. Stuhl, P. Varmazyar, Z. Elekes, Z. Halasz, T. Gilinger, M. Fule, M. Karnok, E. Buzas, A. P. Kovacs, B. Nagy, A. Mohacsi, B. Bıro, L. Csedreki, A. Fenyvesi, Z. Fulop, Z. Korkulu, I. Kuti, J. Csontos, P. P. Geetha, S. Toth, G. Szabo, and K. Osvay, "Continuous high-yield fast neutron generation with few-cycle laser pulses at 10 Hz for applications," Phys. Rev. Res. **7**, 023137 (2025).
[74]C. W. Siders, A. J. Bayramian, K. D. Chesnut, A. C. Erlandson, E. Feigenbaum, T. C. Galvin, W. A. Molander, H. T. Nguyen, M. L. Rehak, P. A. Rosso, E. F. Sistrunk, K. I. Schaffers, T. M. Spinka, and C. L. Haefner, "New architectures for PW-scale high peak power lasers scalable to near-MW average powers," Technical Report No. LLNL-CONF-747093, 2018.

[75]J. Kawanaka, N. Miyanaga, H. Azechi, T. Kanabe, T. Jitsuno, K. Kondo, Y. Fujimoto, N. Morio, S. Matsuo, Y. Kawakami, R. Mizoguchi, K. Tauchi, M. Yano, S. Kudo, and Y. Ogura, "3.1-kJ chirped-pulse power amplification in the LFEX laser," J. Phys.: Conf. Ser. **112**, 032006 (2008).
[76]L. Obst, S. Göde, M. Rehwald, F.-E. Brack, J. Branco, S. Bock, M. Bussmann, T. E. Cowan, C. B. Curry, F. Fiuza, M. Gauthier, R. Gebhardt, U. Helbig, A. Huebl, U. Hübner, A. Irman, L. Kazak, J. B. Kim, T. Kluge, S. Kraft, M. Loeser, J. Metzkes, R. Mishra, C. Rödel, H.-P. Schlenvoigt, M. Siebold, J. Tiggesbäumker, S. Wolter, T. Ziegler, U. Schramm, S. H. Glenzer, and K. Zeil, "Efficient laser-driven proton acceleration from cylindrical and planar cryogenic hydrogen jets," Sci. Rep. **7**, 10248 (2017).
[77]U.S. Department of Energy's Office of Fusion Energy Sciences (FES), LaserNetUS, 2023, available at: https://lasernetus.org/.
[78]S. C. Vogel, J. C. Fernandez, D. C. Gautier, N. Mitura, M. Roth, and K. F. Schoenberg, "Short-pulse laser-driven moderated neutron source," EPJ Web Conf. **231**, 01008 (2020).
[79]Y. Yamagata, K. Hirota, J. Ju, S. Wang, S.-y. Morita, J.-i. Kato, Y. Otake, A. Taketani, Y. Seki, M. Yamada, H. Ota, U. Bautista, and Q. Jia, "Development of a neutron generating target for compact neutron sources using low energy proton beams," J. Radioanal. Nucl. Chem. **305**, 787–794 (2015).
[80]Y. Otake, Y. Seki, Y. Wakabayashi, Y. Ikeda, T. Hashiguchi, Y. Yoshimura, H. Sunaga, A. Taketani, M. Mizuta, Y. Oshima, and M. Ishida, "Research and development of a non-destructive inspection technique with a compact neutron source," J. Disaster Res. **12**, 585–592 (2017).
[81]P. Xu, Y. Ikeda, T. Hakoyama, M. Takamura, Y. Otake, and H. Suzuki, "In-house texture measurement using a compact neutron source," J. Appl. Crystallogr. **53**, 444–454 (2020).
[82]S. Alzubaidi, U. Bartz, M. Basten, A. Bechtold, L. P. Chau, C. Claessens, H. Dinter, M. Droba, C. Fix, H. Hähnel, M. Heilmann, O. Hinrichs, S. Huneck, B. Klump, M. Lotz, D. Mäder, O. Meusel, D. Noll, T. Nowottnick, M. Obermayer, O. Payir, N. Petry, H. Podlech, U. Ratzinger, A. Schempp, S. Schmidt, P. Schneider, A. Seibel, M. Schwarz, W. Schweizer, K. Volk, C. Wagner, and C. Wiesner, "The Frankfurt neutron source FRANZ," Eur. Phys. J. Plus **131**, 124 (2016).
[83]G. Russell, C. Bowman, E. Whitaker, H. Robinson, and M. Meier, "LANSCE high-power (200 mA) target-moderator-reflector-shield," in *ICANS-VIII: Proceedings of the Eighth Meeting of the International Collaboration on Advanced Neutron Sources* (IEEE, 1985), pp. 272–293.
[84]M. Zimmer, S. Scheuren, A. Kleinschmidt, N. Mitura, A. Tebartz, G. Schaumann, T. Abel, T. Ebert, M. Hesse, Ş. Zähter, S. C. Vogel, O. Merle, R.-J. Ahlers, S. Duarte Pinto, M. Peschke, T. Kröll, V. Bagnoud, C. Rödel, and M. Roth, "Demonstration of non-destructive and isotope-sensitive material analysis using a short-pulsed laser-driven epi-thermal neutron source," Nat. Commun. **13**, 1173 (2022).
[85]J. Alvarez, J. Fernández-Tobias, K. Mima, S. Nakai, S. Kar, Y. Kato, and J. Perlado, "Laser driven neutron sources: Characteristics, applications and prospects," Phys. Procedia **60**, 29–38 (2014), part of Special Issue: 3rd International Meeting of the Union for Compact Accelerator-driven Neutron Sources, UCANS III, 31 July–3 August 2012, Bilbao, Spain & the 4th International Meeting of the Union for Compact Accelerator-driven Neutron Sources, UCANS IV, 23–27 September 2013, Sapporo, Hokkaido, Japan.
[86]Phoenix Neutron Imaging Center, PhoenixLLC, 2023), available at: https://www.phoenixneutronimaging.com/.
[87]Neutron Imaging and Applied Materials, PSI AMG, 2023, available at: https://www.psi.ch/de/niag/industrial-services.
[88]Y. Wakabayashi, T. Hashiguchi, Y. Yoshimura, M. Mizuta, Y. Ikeda, and Y. Otake, "Study of a collimation method as a nondestructive diagnostic technique by PGNAA for salt distribution in concrete structures at RANS," EPJ Web Conf. **231**, 05007 (2020).
[89]T. T. Jäger, T. Y. Hirsh, S. Scheuren, A. M. Long, A. S. Losko, A. Wolfertz, M. Zimmer, M. Roth, and S. C. Vogel, "Characterization of a mock up nuclear waste package using energy resolved MeV neutron analysis," Sci. Rep. **15**, 6823 (2025).
[90]A. Yogo, S. R. Mirfayzi, Y. Arikawa, Y. Abe, T. Wei, T. Mori, Z. Lan, Y. Hoonoki, D. O. Golovin, K. Koga, Y. Suzuki, M. Kanasaki, S. Fujioka, M. Nakai, T. Hayakawa, K. Mima, H. Nishimura, S. Kar, and R. Kodama, "Single shot radiography by a bright source of laser-driven thermal neutrons and x-rays," Appl. Phys. Express **14**, 106001 (2021).
[91]J. J. Li, B. Yu, T. Xu, Z. J. Chen, J. H. Zheng, L. Yao, Y. S. Dong, and J. M. Yang, "First magnifying neutron/x-ray combined radiography at Shenguang laser facility," AIP Adv. **12**, 115012 (2022).
[92]C. M. Brenner, S. R. Mirfayzi, D. R. Rusby, C. Armstrong, A. Alejo, L. A. Wilson, R. Clarke, H. Ahmed, N. M. H. Butler, D. Haddock, A. Higginson, A. McClymont, C. Murphy, M. Notley, P. Oliver, R. Allott, C. Hernandez-Gomez, S. Kar, P. McKenna, and D. Neely, "Laser-driven x-ray and neutron source development for industrial applications of plasma accelerators," Plasma Phys. Controlled Fusion **58**, 014039 (2015).
[93]F. Treffert, M. Aufderheide, J. Bendahan, M. P. Hill, T. Ma, D. R. Rusby, M. P. Selwood, and G. J. Williams, "Platform development toward ultra-intense laser-based simultaneous hard x-ray and MeV neutron multimodal radiography," Rev. Sci. Instrum. **95**, 123305 (2024).
[94]L. Zechen and Y. Akifumi, "Exploring nuclear photonics with a laser driven neutron source," Plasma Phys. Controlled Fusion **64**, 024001 (2021).
[95]A. S. Tremsin, W. Kockelmann, D. E. Pooley, and W. B. Feller, "Spatially resolved remote measurement of temperature by neutron resonance absorption," Nucl. Instrum. Methods Phys. Res., Sect. A **803**, 15–23 (2015).
[96]R. Woracek, J. Santisteban, A. Fedrigo, and M. Strobl, "Diffraction in neutron imaging—A review," Nucl. Instrum. Methods Phys. Res., Sect. A **878**, 141–158 (2018).
[97]S. Vogel, "A rietveld-approach for the analysis of neutron time-of-flight transmission data," Ph.D. dissertation (Christian-Albrechts Universität, Kiel, 2000).
[98]R. Woracek, D. Penumadu, N. Kardjilov, A. Hilger, M. Boin, J. Banhart, and I. Manke, "3D mapping of crystallographic phase distribution using energy-selective neutron tomography," Adv. Mater. **26**, 4069–4073 (2014).
[99]A. W. T. Gregg, J. N. Hendriks, C. M. Wensrich, A. Wills, A. S. Tremsin, V. Luzin, T. Shinohara, O. Kirstein, M. H. Meylan, and E. H. Kisi, "Tomographic reconstruction of two-dimensional residual strain fields from Bragg-edge neutron imaging," Phys. Rev. Appl. **10**, 064034 (2018).
[100]A. S. Tremsin, J. Rakovan, T. Shinohara, W. Kockelmann, A. S. Losko, and S. C. Vogel, "Non-destructive study of bulk crystallinity and elemental composition of natural gold single crystal samples by energy-resolved neutron imaging," Sci. Rep. **7**, 40759 (2017).
[101]A. S. Tremsin, S. C. Vogel, M. Mocko, M. A. M. Bourke, V. Yuan, R. O. Nelson, D. W. Brown, and W. B. Feller, "Non-destructive studies of fuel pellets by neutron resonance absorption radiography and thermal neutron radiography," J. Nucl. Mater. **440**, 633–646 (2013).
[102]A. S. Tremsin, A. S. Losko, S. C. Vogel, D. D. Byler, K. J. McClellan, M. A. M. Bourke, and J. V. Vallerga, "Non-contact measurement of partial gas pressure and distribution of elemental composition using energy-resolved neutron imaging," AIP Adv. **7**, 015315 (2017).
[103]A. S. Tremsin, D. Perrodin, A. S. Losko, S. C. Vogel, M. A. M. Bourke, G. A. Bizarri, and E. D. Bourret, "Real-time crystal growth visualization and quantification by energy-resolved neutron imaging," Sci. Rep. **7**, 46275 (2017).
[104]A. S. Losko and S. C. Vogel, "3D isotope density measurements by energy-resolved neutron imaging," Sci. Rep. **12**, 6648 (2022).
[105]S. R. Mirfayzi, A. Yogo, Z. Lan, T. Ishimoto, A. Iwamoto, M. Nagata, M. Nakai, Y. Arikawa, Y. Abe, D. Golovin, Y. Honoki, T. Mori, K. Okamoto, S. Shokita, D. Neely, S. Fujioka, K. Mima, H. Nishimura, S. Kar, and R. Kodama, "Proof-of-principle experiment for laser-driven cold neutron source," Sci. Rep. **10**, 20157 (2020).
[106]A. Wolfertz, A. Losko, A. M. Long, S. Brodish, A. E. Craft, A. Khaplanov, S. C. Vogel, R. O. Nelson, S. A. Wender, A. Tremsin, T. Y. Hirsh, T. T. Jäger, M. Morgano, and P. Feng, "Energy-resolved fast-neutron radiography using an event-mode neutron imaging detector," Sci. Rep. **14**, 30487 (2024).
[107]P. Schillebeeckx, B. Becker, Y. Danon, K. Guber, H. Harada, J. Heyse, A. R. Junghans, S. Kopecky, C. Massimi, M. C. Moxon, N. Otuka, I. Sirakov, and K. Volev, "Determination of resonance parameters and their covariances from neutron induced reaction cross section data," Nucl. Data Sheets **113**, 3054–3100 (2012).
[108]W. Mondelaers and P. Schillebeeckxx, "GELINA, a neutron time-of-flight facility for high-resolution neutron data measurements," Not. Neutroni Luce Sincrotrone **11**, 19 (2006).

[109]B. Martinez, S. N. Chen, S. Bolaños, N. Blanchot, G. Boutoux, W. Cayzac, C. Courtois, X. Davoine, A. Duval, V. Horny, I. Lantuejoul, L. Le Deroff, P. E. Masson-Laborde, G. Sary, B. Vauzour, R. Smets, L. Gremillet, and J. Fuchs, "Numerical investigation of spallation neutrons generated from petawatt-scale laser-driven proton beams," Matter Radiat. Extremes **7**, 024401 (2021).
[110]S. N. Chen, F. Negoita, K. Spohr, E. d'Humières, I. Pomerantz, and J. Fuchs, "Extreme brightness laser-based neutron pulses as a pathway for investigating nucleosynthesis in the laboratory," Matter Radiat. Extremes **4**, 054402 (2019).
[111]V. W. Yuan, J. D. Bowman, D. J. Funk, G. L. Morgan, R. L. Rabie, C. E. Ragan, J. P. Quintana, and H. L. Stacy, "Shock temperature measurement using neutron resonance spectroscopy," Phys. Rev. Lett. **94**, 125504 (2005).
[112]D. P. Higginson, J. M. McNaney, D. C. Swift, T. Bartal, D. S. Hey, R. Kodama, S. Le Pape, A. Mackinnon, D. Mariscal, H. Nakamura, N. Nakanii, K. A. Tanaka, and F. N. Beg, "Laser generated neutron source for neutron resonance spectroscopy," Phys. Plasmas **17**(10), 100701 (2010).
[113]J. C. Fernández, C. W. Barnes, M. J. Mocko, and L. Zavorka, "Requirements and sensitivity analysis for temporally- and spatially-resolved thermometry using neutron resonance spectroscopy," Rev. Sci. Instrum. **90**, 094901 (2019).
[114]I. Kishon, A. Kleinschmidt, V. A. Schanz, A. Tebartz, O. Noam, J. C. Fernandez, D. C. Gautier, R. P. Johnson, T. Shimada, G. A. Wurden, M. Roth, and I. Pomerantz, "Laser based neutron spectroscopy," Nucl. Instrum. Methods Phys. Res., Sect. A **932**, 27–30 (2019).
[115]A. Yogo, Z. Lan, Y. Arikawa, Y. Abe, S. R. Mirfayzi, T. Wei, T. Mori, D. Golovin, T. Hayakawa, N. Iwata, S. Fujioka, M. Nakai, Y. Sentoku, K. Mima, M. Murakami, M. Koizumi, F. Ito, J. Lee, T. Takahashi, K. Hironaka, S. Kar, H. Nishimura, and R. Kodama, "Laser-driven neutron generation realizing single-shot resonance spectroscopy," Phys. Rev. X **13**, 011011 (2023).
[116]Z. Lan, Y. Arikawa, S. R. Mirfayzi, A. Morace, T. Hayakawa, H. Sato, T. Kamiyama, T. Wei, Y. Tatsumi, M. Koizumi, Y. Abe, S. Fujioka, K. Mima, R. Kodama, and A. Yogo, "Single-shot laser-driven neutron resonance spectroscopy for temperature profiling," Nat. Commun. **15**, 5365 (2024).
[117]D. D. Das, N. Sharma, and P. A. Chawla, "Neutron activation analysis: An excellent nondestructive analytical technique for trace metal analysis," Crit. Rev. Anal. Chem. **54**, 2450 (2023).
[118]Y. Toh, M. Ebihara, A. Kimura, S. Nakamura, H. Harada, K. Y. Hara, M. Koizumi, F. Kitatani, and K. Furutaka, "Synergistic effect of combining two nondestructive analytical methods for multielemental analysis," Anal. Chem. **86**, 12030–12036 (2014).
[119]Z. Revay, T. Belya, L. Szentmiklosi, and G. L. Molnár, "Prompt gamma activation analysis using a chopped neutron beam," J. Radioanal. Nucl. Chem. **264**, 277–281 (2005).
[120]V. A. J. van Lint, R. E. Leadon, and J. F. Colwell, "Energy dependence of displacement effects in semiconductors," IEEE Trans. Nucl. Sci. **19**, 181–185 (1972).
[121]S. Wender and L. Dominik, "Los Alamos high-energy neutron testing handbook," SAE Int. J. Adv. Curr. Pract. Mobility **2**, 1279–1302 (2020).
[122]S. E. Michalak, K. W. Harris, N. W. Hengartner, B. E. Takala, and S. A. Wender, "Using the LANSCE irradiation facility to predict the number of fatal soft errors in one of the world's fastest supercomputers," Nucl. Instrum. Methods Phys. Res., Sect. B **241**, 414–418 (2005).
[123]D. M. Fleetwood, "Perspective on radiation effects in nanoscale metal-oxide-semiconductor devices," Appl. Phys. Lett. **121**, 070503 (2022).
[124]T. J. Ruth, "The shortage of technetium-99m and possible solutions," Annu. Rev. Nucl. Part Sci. **70**, 77–94 (2020).
[125]M. Bleuel, M. Siebenbürger, P. Böni, and G. J. Schneider, "A design study of a compact small-angle neutron scattering instrument," arXiv:2201.12930 (2022).
[126]P. Thiyagarajan, J. E. Epperson, R. K. Crawford, J. M. Carpenter, T. E. Klippert, and D. G. Wozniak, "The time-of-flight small-angle neutron diffractometer (SAD) at IPNS, Argonne National Laboratory," J. Appl. Crystallogr. **30**, 280–293 (1997).
[127]European Spallation Source, ESS Instruments, 2023, available at: https://europeanspallationsource.se/instruments.
[128]K. H. Andersen, D. N. Argyriou, A. J. Jackson, J. Houston, P. F. Henry, P. P. Deen, R. Toft-Petersen, P. Beran, M. Strobl, T. Arnold, H. Wacklin-Knecht, N. Tsapatsaris, E. Oksanen, R. Woracek, W. Schweika, D. Mannix, A. Hiess, S. Kennedy, O. Kirstein, S. Petersson Årsköld, J. Taylor, M. E. Hagen, G. Laszlo, K. Kanaki, F. Piscitelli, A. Khaplanov, I. Stefanescu, T. Kittelmann, D. Pfeiffer, R. Hall-Wilton, C. I. Lopez, G. Aprigliano, L. Whitelegg, F. Y. Moreira, M. Olsson, H. N. Bordallo, D. Martín-Rodríguez, H. Schneider, M. Sharp, M. Hartl, G. Nagy, S. Ansell, S. Pullen, A. Vickery, A. Fedrigo, F. Mezei, M. Arai, R. K. Heenan, W. Halcrow, D. Turner, D. Raspino, A. Orszulik, J. Cooper, N. Webb, P. Galsworthy, J. Nightingale, S. Langridge, J. Elmer, H. Frielinghaus, R. Hanslik, A. Gussen, S. Jaksch, R. Engels, T. Kozielewski, S. Butterweck, M. Feygenson, P. Harbott, A. Poqué, A. Schwaab, K. Lieutenant, N. Violini, J. Voigt, T. Brückel, M. Koenen, H. Kämmerling, E. Babcock, Z. Salhi, A. Wischnewski, A. Heynen, S. Désert, J. Jestin, F. Porcher, X. Fabrèges, G. Fabrèges, B. Annighöfer, S. Klimko, T. Dupont, T. Robillard, A. Goukassov, S. Longeville, C. Alba-Simionesco, P. Bourges, J. Guyon Le Bouffy, P. Lavie, S. Rodrigues, E. Calzada, M. Lerche, B. Schillinger, P. Schmakat, M. Schulz, M. Seifert, W. Lohstroh, W. Petry, J. Neuhaus, L. Loaiza, A. Tartaglione, A. Glavic, S. Schütz, J. Stahn, E. Lehmann, M. Morgano, J. Schefer, U. Filges, C. Klauser, C. Niedermayer, J. Fenske, G. Nowak, M. Rouijaa, D. J. Siemers, R. Kiehn, M. Müller, H. Carlsen, L. Udby, K. Lefmann, J. O. Birk, S. Holm-Dahlin, M. Bertelsen, U. B. Hansen, M. A. Olsen, M. Christensen, K. Iversen, N. B. Christensen, H. M. Rønnow, P. G. Freeman, B. C. Hauback, R. Kolevatov, I. Llamas-Jansa, A. Orecchini, F. Sacchetti, C. Petrillo, A. Paciaroni, P. Tozzi, M. Zanatta, P. Luna, I. Herranz, O. G. del Moral, M. Huerta, M. Magán, M. Mosconi, E. Abad, J. Aguilar, S. Stepanyan, G. Bakedano, R. Vivanco, I. Bustinduy, F. Sordo, J. L. Martínez, R. E. Lechner, F. J. Villacorta, J. Šaroun, P. Lukáš, M. Markó, M. Zanetti, S. Bellissima, L. del Rosso, F. Masi, C. Bovo, M. Chowdhury, A. De Bonis, L. Di Fresco, C. Scatigno, S. F. Parker, F. Fernandez-Alonso, D. Colognesi, R. Senesi, C. Andreani, G. Gorini, G. Scionti, and A. Schreyer, "The instrument suite of the European Spallation Source," Nucl. Instrum. Methods Phys. Res., Sect. A **957**, 163402 (2020).
[129]T. Brückel, "Technical design report HBS volume 3–Instrumentation," in *Schriften des Forschungszentrums Jülich* (Forschungszentrum Jülich GmbH, Jülich, 2023).
[130]ILL, ILL Instruments, 2023, available at: https://www.ill.eu/users/instruments.
[131]D. V. Baxter, "Materials and neutronics research at the low energy neutron source," Eur. Phys. J. Plus **131**, 83 (2016).
[132]M. Murakami, J. J. Honrubia, K. Weichman, A. V. Arefiev, and S. V. Bulanov, "Generation of megatesla magnetic fields by intense-laser-driven microtube implosions," Sci. Rep. **10**, 16653 (2020).
[133]Compact Accelerator Based Neutron Sources, Ser. TECDOC Series, International Atomic Energy Agency, Vienna, 2021, available at: https://www.iaea.org/publications/14948/compact-accelerator-based-neutron-sources.
[134]A. Kleinschmidt, "Investigation of a laser-driven neutron source with respect to different fields of application," Ph.D. dissertation (Technische Universität Darmstadt, 2017).
[135]M. M. Günther, O. N. Rosmej, P. Tavana, M. Gyrdymov, A. Skobliakov, A. Kantsyrev, S. Zähter, N. G. Borisenko, A. Pukhov, and N. E. Andreev, "Forward-looking insights in laser-generated ultra-intense γ-ray and neutron sources for nuclear application and science," Nat. Commun. **13**, 170 (2022).
[136]S. R. Mirfayzi, A. Alejo, H. Ahmed, D. Raspino, S. Ansell, L. A. Wilson, C. Armstrong, N. M. H. Butler, R. J. Clarke, A. Higginson, J. Kelleher, C. D. Murphy, M. Notley, D. R. Rusby, E. Schooneveld, M. Borghesi, P. McKenna, N. J. Rhodes, D. Neely, C. M. Brenner, and S. Kar, "Experimental demonstration of a compact epithermal neutron source based on a high power laser," Appl. Phys. Lett. **111**, 044101 (2017).
[137]M. Angelone and C. Verona, "Properties of diamond-based neutron detectors operatedin harsh environments," J. Nucl. Eng. **2**, 422–470 (2021).
[138]A. S. Losko, Y. Han, B. Schillinger, A. Tartaglione, M. Morgano, M. Strobl, J. Long, A. S. Tremsin, and M. Schulz, "New perspectives for neutron imaging through advanced event-mode data acquisition," Sci. Rep. **11**, 21360 (2021).
[139]I. Mor, D. Vartsky, D. Bar, G. Feldman, M. B. Goldberg, D. Katz, E. Sayag, I. Shmueli, Y. Cohen, A. Tal, Z. Vagish, B. Bromberger, V. Dangendorf, D. Mugai, K. Tittelmeier, and M. Weierganz, "High spatial resolution fast-neutron imaging detectors for pulsed fast neutron transmission spectroscopy," J. Instrum. **4**, P05016 (2009).
[140]League of advanced European Neutron Sources (LENS), Neutron Science in Europe, 2022, available at: https://lens-initiative.org/wp-content/uploads/2022/08/LENS-Report-findoublepages.pdf.